

**Editor Decision: Publish subject to minor revisions (review by Editor) (22 Aug 2016) by Dr Kumiko Goto-Azuma**  
Comments to the Author:  
Dear Dr. Maselli,

**I think you have addressed most of the referee comments. But some of them have not been fully addressed. I have a few comments for further revisions.**

**Q1: As Referee #2 (Ref2 hereafter) commented, using the MSA data to determine the sea ice component of the Br signal is tricky. The substantial negative values of the non-sea-ice Br (Fig. 8) worries me. Can you give any reasonable explanation for the negative values? The large scatter of the data shown in Fig. R6a,b does not look very convincing, either, even though the correlation may be statistically significant. When you did a linear fitting between the MSA and Br data, you used smoothed data only for MSA. Wouldn't it be better if you use smoothed data also for Br?**

R1: The negative values appear during the period when the non-sea ice Br is, on average, zero. The negative values are thus a result of the total Br being less than the smoothed MSA value. Though the sources of Br and MSA are linked – which is what provides the similarities between the general low frequency trend of the two species, the atmospheric processing, transport and deposition of the two species may be modified by different variables such as changes in aerosol acidity, for example. These variables cause the short term differences between the MSA and total Br records preserved in the ice so we believe it is not unreasonable to expect negative values in the calculated non-sea ice Br record when the MSA and total Br are close (essentially no non-sea ice Br).

Only the MSA data was smoothed (as opposed to Br and MSA both being smoothed) to try and minimize the amount of data manipulation in the production of the non-sea ice Br record. However, as can be seen from the Figure Q1 (attached, Summit-2010) a smoothing of the calculated non-sea ice Br record (as shown in the manuscript) produces the same result as if the non-sea ice Br record was calculated from the difference between the smoothed total Br record and the smoothed MSA record. Looking at the smoothed version of the non-sea ice Br record, it is clear that there is a sustained period (1815-1870 C.E.) over which the non-sea ice Br record is on average, below zero. In both the Summit and Tunu ice core sites this period corresponds to a period of significant volcanic activity (including the Tambora eruption of 1815 C.E.) and this may be evidence acid induced loss of total Br, or perhaps a modification on the atmospheric MSA production by the increased sulfate levels. This conclusion is pure speculation; however, it is supported by the observation that the other period of negative non-sea ice Br values in the Tunu record occurring during the period of elevated sulfate levels (~1860-1940 C.E.).

A comment has been added to the manuscript discussing the negative non-sea ice Br values and the possible links to the elevated sulfate values in section 4.2.2.

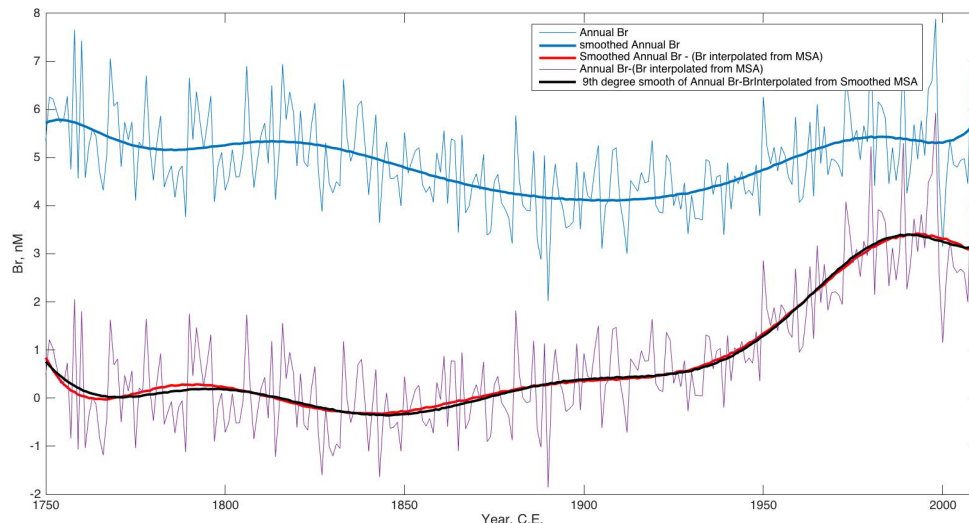


Figure Q1: Summit-2010 non-sea ice bromine (nsiBr; red line) calculated as the difference between the smoothed total bromine record (thick blue line) and the sea ice bromine record interpolated from the smoothed MSA record. For comparison the nsiBr record (thin purple line, as displayed in the manuscript) calculated from the difference between the annual Br (thin blue line) and the sea ice bromine record interpolated from the smoothed MSA record is also shown. The smoothing of the manuscript nsiBr is also shown (thick black line).

**Q2. Both Ref1 and Ref2 commented on biogenic sources of Br. I was also puzzled by the argument on biogenic sources of Br. To me, it is not very clear if the contribution of biogenic sources is important or not. Does the manuscript mean that the sea ice source is dominant in spring and biogenic sources are dominant in summer? Not having read the revised manuscript, I could not evaluate if the manuscript has been revised adequately. Please revise the manuscript carefully to make the logic clear.**

R2. This following text was added to the manuscript in Section 4.1.4. It aims to make clear that the biological sources are not thought to be the major bromine source for the ice core record. “The season of Arctic sea ice algae productivity is confined by limitations in available sunlight and nutrients resulting in a mid-to-late spring maxima – depending upon site location (Leu et al., 2015) – as is reflected in the seasonality of the MSA record. Direct transport of bromine enriched aerosols from these algal sources to the ice core sites again cannot explain the summer maximum of bromine observed in the ice. In addition to the incoherence of the seasonality of the bromine ice core signal, to-date biogenic sources have been considered insignificant sources of bromine in the Arctic marine boundary layer compared with the inorganic bromine source from sea salts (Simpson et al., 2007).”

**Q3. The “3 step linear regression” is explained in author’s response to Ref1. Please explain it also in the revised manuscript.**

R3. The explanation has been included in section 3.1

**Q4. Ref1 suggests that a more detailed consideration of potential impacts of acidity on the stability of Br and MSA in ice cores is needed, this has not been fully addressed. Though the authors argue that they analyzed the discrete samples obtained from the**

**melt stream, this does not address the Ref1's concern about a possibility that MSA might get destabilized at the melt head. Potential impacts of acidity variability within each ice core should be discussed, too, to fully address the Ref1 comment.**

R4. The most conclusive way to determine whether there is destabilization of MSA at the CFA melter head would be to perform discrete MSA analyses on subsamples of the unmelted ice core directly and compare this with the discrete samples obtained at the end of the melt stream. However, this was not performed for this study. Instead we use the comparison between the MSA record generated from the Legrand GRIP ice core (collected only 35 km from the Summit-2010 site) to demonstrate that both techniques measured the same MSA concentrations which suggests no MSA is lost at the melt head. The same conclusion can be reached by comparison to the results of the Summit snow pit study by Jaffrezo et al., (1994). Over the period of winter 1984-1992 Jaffrezo measured MSA concentrations between ~1 and 5 ppb, with a mean of  $2.1 \pm 1.8(1\sigma)$  ppb (calculated from a digitized version of the snowpit data). The annual measurements on the Summit-2010 ice core averaged  $2.0 \pm 0.7(1\sigma)$  ppb over the 1984-1992 period; comparable concentrations to the Jaffrezo study albeit with a lower variability. The comparison between the Legrand, Jaffrezo and Summit-2010 ice core MSA results have been discussed in the Manuscript in section 3.2 and the text box of Figure S4.

Also, it is unlikely that MSA is 'destabilized' at the CFA melter head for several reasons;

- MSA is very chemically stable, only reacting with highly oxidizing species such as the OH radical.
- No OH radicals are produced at the melter head.  $H_2O_2$  records from ice cores have been successfully measured using the continuous melt technique. If the OH radicals were produced at the melter head, then measurements of  $H_2O_2$  in the ice cores would not be possible.
- The CFA melter head is made of chemically inert Silicon Carbide, so there are unlikely to be any surface catalyzed reactions.
- The melter head is only heated to ambient temperatures so no thermal degradation of the MSA is expected.

The acidic variability within the ice cores is unlikely to affect the measurement of the MSA ice core record for several reasons:

- As discussed in the manuscript, the snow accumulation is large enough at both ice core sites that the amount of (acid induced) post-depositional loss of MSA is negligible.
- The MSA measurements were made on ice from the center of the ice core. No MSA is expected to be lost from the center of the ice cores during storage as there is no atmospheric exposure to the central ice.
- The internal isotopomer standard used as part of the MSA measurements would correct for any changes in instrument response due to variations in water chemistry.

**EC1: In Section 2.1, Fig. 1 needs to be referred to.**

REC1: reference to figure 1 has been included in Section 2.1

**EC2. The order of the figures or figure numbers should be re-organized. For example, Fig. 3 is referred to before Fig.2, and Fig.S3 before S1 and S2 (line 173) . Please check the figure numbers and the order that they are referred to.**

REC2. The figures have either been relabeled or the order to which they are referred in the text corrected.

**EC3. The legend for the blue color in Fig.8a reads exPb (x2 after 1925). Does this mean “after 1940?”**

REC3. Figure 8 has been modified for clarity– now there are only the ‘exPb’ and ‘Br from leaded fuel’ time-series. In the figure text box it explains that the ‘Br from leaded fuel’ time-series is created by assuming a 1:1 ratio between exPb and Br from fuel before 1925 and 1:2 ratio after 1925.

**EC4. Line 923. Delete one of the two “significant”s.**

REC4: Correction made

**EC5. Figure 5. Pink circles and the fonts beside the color bar are too small to see. Same applies to some of the other figures and supplementary figures. In some of the figures, legends, axis labels etc. are too small to see. Please make them larger.**

REC5. Figure 5 and S8 circles and color bar fonts increased in size. Figs 6,7 font size increased. All newly added plots have been checked for font size.

#### References:

Jaffrezo, J. L., Davidson, C. I., Legrand, M. and Dibb, J. E.: Sulfate and MSA in the air and snow on the Greenland Ice Sheet, *J. Geophys. Res.*, 99(D1), 1241–1253, doi:10.1029/93JD02913, 1994.

Leu, E., Mundy, C. J., Assmy, P., Campbell, K., Gabrielsen, T. M., Gosselin, M., Juul-Pedersen, T. and Gradinger, R.: Arctic spring awakening - Steering principles behind the phenology of vernal ice algal blooms, *Prog. Oceanogr.*, 139, 151–170, doi:10.1016/j.pocean.2015.07.012, 2015.

Simpson, W. R., von Glasow, R., Riedel, K., Anderson, P., Ariya, P., Bottenheim, J., Burrows, J., Carpenter, L. J., Friess, U., Goodsite, M. E., Heard, D., Hutterli, M., Jacobi, H.-W., Kaleschke, L., Neff, B., Plane, J., Platt, U., Richter, a., Roscoe, H., Sander, R., Shepson, P., Sodeau, J., Steffen, a., Wagner, T. and Wolff, E.: Halogens and their role in polar boundary-layer ozone depletion, , 4375–4418, doi:10.5194/acpd-7-4285-2007, 2007.



1 **Sea ice and pollution-modulated changes in Greenland ice core**  
2 **methanesulfonate and bromine**

3 **O.J. Maselli<sup>1\*</sup>, N.J. Chellman<sup>1</sup>, M. Grieman<sup>2</sup>, L. Layman<sup>1</sup>, J. R. McConnell<sup>1</sup>, D. Pasteris<sup>1</sup>,**  
4 **R.H. Rhodes<sup>3</sup>, E. Saltzman<sup>2</sup>, M. Sigl<sup>1</sup>**

5 [1] {Desert Research Institute, Department of Hydrologic Sciences, Reno, NV, USA}

6 [2] {University of California Irvine, Department of Earth System Science, Irvine, CA, USA}

7 [3] {University of Cambridge, Department of Earth Sciences, Cambridge, UK}

8 [\*] {now at: The University of Adelaide, Australia, 5000}

9 *Correspondence to:* Olivia Maselli (olivia.maselli@adelaide.edu.au)

10

11 Keywords: bromine, MSA, nitrate, sea ice, pollution, acidification, Arctic, Greenland, cryosphere

12

13 **Abstract**

14 Reconstruction of past changes in Arctic sea ice extent may be critical for understanding its future  
15 evolution. Methanesulphonate (MSA) and bromine concentrations preserved in ice cores have both  
16 been proposed as indicators of past sea ice conditions. In this study, two ice cores from central and NE  
17 Greenland were analysed at sub-annual resolution for MSA ( $CH_3SO_3H$ ) and bromine, covering the time  
18 period 1750-2010. We examine correlations between ice core MSA and the HadISST1 ICE sea ice  
19 dataset and consult back-trajectories to infer the likely source regions. A strong correlation between the  
20 low frequency MSA and bromine records during preindustrial times indicates that both chemical species  
21 are likely linked to processes occurring on or near sea ice in the same source regions. The positive  
22 correlation between ice core MSA and bromine persists until the mid-20th century, when the acidity of  
23 Greenland ice begins to increase markedly due to increased fossil fuel emissions. After that time, MSA  
24 levels decrease as a result of declining sea ice extent but bromine levels increase. We consider several  
25 possible explanations and ultimately suggest that increased acidity, specifically nitric acid, of snow on  
26 sea ice stimulates the release of reactive Br from sea ice, resulting in increased transport and deposition  
27 on the Greenland ice sheet.

29 **1 Introduction**

30 Atmospheric chemistry in the polar regions is strongly modulated by physical, chemical, and biological  
 31 processes occurring in and around sea ice. These include sea salt aerosol generation, biogenic emissions  
 32 of sulfur-containing gases and halogenated organics, and the photochemical/heterogeneous reactions  
 33 leading to release of volatile, reactive bromine species. The resulting chemical signals influence the  
 34 chemistry of the aerosol deposited on polar ice sheets. For this reason ice core measurements of sea salt  
 35 ions, methanesulphonate (MSA), and bromine have been examined as potential tracers for sea ice extent  
 36 (Abram et al., 2013; Spolaor et al., 2013b, 2016; Wolff et al., 2003). The interpretation of such tracers  
 37 is complicated by the fact that their source functions reflect changes in highly complex systems, and  
 38 signals are further modified by patterns of atmospheric transport and deposition.

39 MSA is produced by the atmospheric oxidation of DMS ( $(CH_3)_2S$ ). DMS is produced throughout the  
 40 world's oceans as a breakdown product of the algal metabolite DMSP,  $((CH_3)_2S^+CH_2CH_2COO^-)$ .  
 41 DMS emissions are particularly strong in marginal sea ice zones (Sharma et al., 2012), and this source  
 42 is believed to be a dominant contributor to the MSA signal in polar ice (Curran and Jones, 2000). Ice  
 43 core MSA records have been used extensively in Antarctica as a proxy for local sea ice dynamics.  
 44 Although the specifics of the relationship are highly site-dependent (Abram et al., 2013; Curran et al.,  
 45 2003) MSA has been proven to be a reasonably good proxy for sea ice conditions (e.g., (Curran and  
 46 Jones, 2000)). In the Arctic, the relationship between MSA and sea ice conditions is less straightforward  
 47 due to the likelihood of multiple source regions with different sea ice conditions contributing to the ice  
 48 core archived MSA (Abram et al., 2013). Until now, a significant, ( $r = -0.66$ ) relationship between ice  
 49 core MSA and Arctic sea ice extent (specifically August in the Barents sea) has only been established  
 50 for a short record from a Svalbard ice core (O'Dwyer et al., 2000). In this study we analyse the direct  
 51 correlations between the MSA records from two Greenland ice core sites and the surrounding sea ice  
 52 conditions in order to demonstrate the utility of MSA as a local sea ice proxy.

53 In this study, all dissolved or suspended bromine species are measured (including organic bromine) and  
 54 shall be referred to as "bromine". The primary source of total inorganic bromine (e.g.  $Br_2$ ,  $Br^-$ ,  $HBr$ )  
 55 in the marine boundary layer (MBL) is the ocean (Parrella et al., 2012; Sander et al., 2003). At  
 56 concentrations of less than 0.2% that of sodium (Na), bromide ( $Br^-$ ) makes a small contribution to  
 57 ocean salinity.  $Br^-$  can be concentrated in the high latitude oceans when the sea water is frozen, since  
 58 the formation of the ice matrix exudes the sea-salts in the form of brine (Abbatt et al., 2012). Small, sea-  
 59 salt aerosol particles blown from the surface of sea ice are typically enriched with bromine (Sander et

Deleted: ph

Deleted: but rather weak

Deleted: 37

Deleted: c

Deleted: (Parrella et al., 2012; Sander et al., 2003)

al., 2003), and satellite imagery has revealed that plumes of bromine (as BrO) are photo-chemically released from sea-ice zones in spring (Nghiem et al., 2012; Schönhardt et al., 2012; Wagner et al., 2001). Recently, studies have begun to link ice core records of bromide enrichment (relative to sea water Na concentrations) preserved in polar ice sheets to that of local sea ice conditions (Spolaor et al., 2013a, 2013b, 2014). Spolaor and co-workers demonstrated the spring-time  $Br^-/Na$  that is preserved in the ice core is a record of bromine explosion events over adjacent seasonal sea ice. A  $Br^-/Na$  enrichment would therefore indicate a larger seasonal sea ice extent or conversely a shorter distance between the ice edge and the ice core site due to decreased multi-year sea ice (Spolaor et al., 2013a). However, like MSA, it is likely that the bromine – sea-ice relationship in the Arctic is complicated by the myriad of bromine source regions which influence an ice core record in addition to factors which influence the degree of enrichment of the aerosol as it travels to the ice core site. In this study we compare ice core records of bromine to those of MSA and other common MBL species in order to determine the influence of sea ice conditions and other factors on bromine concentrations.

Here we present measurements of MSA, bromine, and elemental tracers of sea salt and crustal input in two Greenland ice cores covering the time period 1750-2010 C.E.. These ice core records represent the first continuous, sub-annual resolution records of bromine in polar ice to extend beyond the satellite era. We examine the relationship between these two sea ice-modulated tracers, their relationship to independent historical estimates of sea ice distribution, and the influence of industrialization on atmospheric and ice core chemistry.

## 2 Methods

### 2.1 Ice cores

The 87 m ‘Summit-2010’ ice core was collected in 2010 close to Summit Station, Greenland (72°20'N 38°17'24"W, Fig. 1). The average snow accumulation at Summit is ~0.22 m yr<sup>-1</sup> water equivalent, with few instances of melt. Due to the relatively high snow accumulation rate, seasonal analysis of the sea salt species concentrations was feasible. The 213 m Tunu core was collected in 2013 (78° 2' 5.5"N, 33° 52' 48"W, Fig. 1), approximately 3 km east of the Tunu-N automatic weather station, part of the Greenland Climate Network. The average snow accumulation at Tunu is ~0.11 m yr<sup>-1</sup> water equivalent. The Summit-2010 and Tunu cores were dated using well-known volcanic horizons in sulfur (S). The dating of Summit-2010 was refined by annual layer counting using seasonal cycles in the ratio of non-sea salt S/Na (Sigl et al., 2015). The error in the dating of the ice core records was estimated as ± 0.33 years for the Summit-2010 record and ± 1 years for the Tunu record.

Deleted: (Sander et al., 2003)

## 2.2 Sampling and analysis

The ice cores were sampled from 33x33 mm cross-section sticks using a continuous melter system (McConnell et al., 2002). The silicon carbide melter plate provides three streams from concentric square regions of the ice core sample: an innermost stream (with a cross sectional area of 144 mm<sup>2</sup>), an intermediate stream (340 mm<sup>2</sup>) and an outer stream that was discarded along with any contaminants obtained from handling of the ice core. The innermost melt stream was directed to two inductively coupled plasma-mass spectrometers (ICP-MS, Thermo Element II high resolution with PFA-ST concentric Teflon nebulizer (ESI)) run in parallel. All calibrations and runtime standards were run on both instruments and several elements were also measured in duplicate (Na, Ce, Pb) to ensure tracking between both ICP-MS. In addition, an internal standard of yttrium flowed through the entire analytical system and was used to observe any change in system sensitivity. The instrument measuring bromine was run at medium resolution and there were no mass interferences observed at the bromine isotope mass monitored (79 amu). The sample stream was acidified to 1% *HNO*<sub>3</sub> to prevent loss of less soluble species, degassed just prior to analysis to minimize mixing in the sample line and sampled at a rate of 0.45 ml min<sup>-1</sup> (McConnell et al., 2002; Sigl et al., 2013). The following elements were measured by ICP-MS: Br, Cl, Na, Ca, S, Ce, and Pb. Calibration of the ICP-MS was based on a series of 7 mixed standards measured at the start and end of each day for all elements except for the halides. Due to the high volatility of acid halides, a set of 4 bromine and chlorine standards were made individually in a 1% UHP *HNO*<sub>3</sub> matrix from fresh, non-acidified intermediate stock solution (Inorganic Ventures) every day. The intermediate melt stream was directed to a continuous flow analysis (CFA) system on which nitrate ion (*NO*<sub>3</sub><sup>-</sup>) and snow acidity (sum of soluble acidic species) were measured using the technique described by Pasteris (2012) in addition to other atmospheric species of interest (Röthlisberger et al., 2000).

A portion of the debubbled CFA melt stream (150 µl min<sup>-1</sup>) was subsampled using a peristaltic pump for continuous on-line analysis of methanesulfonate by electrospray triple-quad mass spectrometer (ESI/MS/MS; Thermo-Finnigan Quantum). This subsample was mixed with pure methanol (50 µl min<sup>-1</sup>) delivered using an M6 pump (VICI). The methanol was spiked with an internal standard of deuterated MSA (*CD*<sub>3</sub>*SO*<sub>3</sub><sup>-</sup>; Cambridge Isotopes) at a concentration of 52 nM. The internal isotope standard was used to correct for any changes in instrument response due to variations in water chemistry (such as acidity). The isotope standard was calibrated against non-deuterated MSA standards prepared in water from non-deuterated MSA (*CH*<sub>3</sub>*SO*<sub>3</sub><sup>-</sup>; Sigma Aldrich). MSA was detected in negative ion mode using the *CH*<sub>3</sub>*SO*<sub>3</sub><sup>-</sup>/*SO*<sub>3</sub><sup>-</sup> transition (*m/z* 95/80) and *CD*<sub>3</sub>*SO*<sub>3</sub><sup>-</sup>/*SO*<sub>3</sub><sup>-</sup> (*m/z* 98/80). The concentration of MSA in the sample flow was determined from the ratio of the non-deuterated and deuterated signals after minor

Deleted:

Deleted: low

Deleted: to get the highest sensitivity

blank corrections. The analysis of MSA by batch analysis using ESI/MS/MS has been reported previously (Saltzman et al., 2006). This study is the first use of the technique for ice core MSA analysis in a continuous, online mode. The uncertainty in the MSA intensity as calculated from the standard calibrations is 1%.

Deleted: on-line

A second portion of the debubbled CFA melt stream was directed to an autosampler collection system to collect a discretely sampled archive of the melted ice cores. The collected samples were frozen at the end of each day and later analysed for MSA again using ion chromatography and ESI/MS/MS.

### 2.3 Calculation of anthropogenic Pb, non sea-salt S, and Br enrichment

Deleted:

The Pb derived from anthropogenic sources (exPb) was calculated as the difference between total lead and that from dust sources:

$$\text{exPb} = [\text{Pb}]_{\text{obs}} - [\text{Ce}]_{\text{obs}} \times \left( \frac{[\text{Pb}]}{[\text{Ce}]} \right)_{\text{dust}} \quad (1)$$

Deleted:  $\text{exPb} = [\text{Pb}]_{\text{obs}} - [\text{Ce}]_{\text{obs}} \times \left( \frac{[\text{Pb}]}{[\text{Ce}]} \right)_{\text{dust}}$

Formatted: Font:Bold

Formatted: Font:12 pt

Formatted: Normal, Tabs:Not at 16.5 cm

Deleted:  $([\text{Pb}]/[\text{Ce}])_{\text{dust}}$

Deleted:

Deleted: ph

Formatted: Font:10 pt

Formatted: Font:10 pt

Formatted: Font:10 pt

Formatted: Font:10 pt

Formatted: Font:10 pt

Deleted:  $\left( \frac{[\text{SO}_4^{2-}]}{[\text{Na}]} \right)_{\text{seawater}}$

Deleted:  $\text{ssNa} = \frac{[\text{Na}_{\text{obs}} \times R_t - \text{Ca}_{\text{obs}}]}{[R_t - R_m]}$

Where the  $([\text{Pb}]/[\text{Ce}])_{\text{dust}}$  mass ratio has the constant value of 0.20588 (Bowen, 1979).

Similarly the amount of non-sea salt sulfur (nssS) was calculated relative to the sea-salt sodium, ssNa:

$$\text{nssS} = [\text{S}]_{\text{obs}} - [\text{ssNa}] \times \left( \frac{[\text{SO}_4^{2-}]}{[\text{Na}]} \right)_{\text{seawater}} \quad (2)$$

Where the  $\left( \frac{[\text{SO}_4^{2-}]}{[\text{Na}]} \right)_{\text{seawater}}$  mass ratio has the constant value of 0.252 (Millero, 1974). ssNa was calculated by comparison with calcium as both have sea salt and dust origins (Röthlisberger et al., 2002):

$$\text{ssNa} = \frac{[\text{Na}_{\text{obs}} \times R_t - \text{Ca}_{\text{obs}}]}{[R_t - R_m]} \quad (3)$$

Where  $R_t$  and  $R_m$  are the Ca/Na mean crustal and mean marine mass ratios of 1.78 and 0.038, respectively, (Millero, 1974).

Bromine enrichment factors relative to sea water concentrations were calculated using the following:

$$\text{Br}_{\text{enrich}} = \left( \frac{[\text{Br}]}{[\text{Na}]} \right)_{\text{obs}} / \left( \frac{[\text{Br}]}{[\text{Na}]} \right)_{\text{seawater}} \quad (4)$$

Deleted:  $\text{Br}_{\text{enrich}} = \left( \frac{[\text{Br}]}{[\text{Na}]} \right)_{\text{obs}} / \left( \frac{[\text{Br}]}{[\text{Na}]} \right)_{\text{seawater}}$

Formatted: Font:10 pt

where the  $([\text{Br}]/[\text{Na}])_{\text{seawater}}$  mass ratio is 0.00623 (Millero, 1974).

167

2.4 Air mass back trajectories

168

169

170

171

172

173

174

175

176

177

178

2.5 Sea Ice Correlation mapping

179

180

181

182

183

184

185

186

187

188

189

190

191

192

193

194

195

196

197

Outliers were removed from the MSA time series (see Fig. 2) before the correlations were performed using the technique described by Sigl (2013) for identifying volcanic signals using a 25 year running average filter. Correlations were performed on an annual rather than seasonal basis because the seasonality of ice core MSA is distorted due to post-depositional migration of MSA signal at depth in the snow pack (Mulvaney et al., 1992) (Fig. 3, S1).

Deleted: -

Deleted: -

Deleted:

Deleted: -

Formatted: English (AUS)

Deleted: 3.4

Moved down [1]: depositional migration of MSA signal at depth in the snow pack (Mulvaney et al., 1992) (Fig. 3,

Deleted: Correlations were performed on an annual rather than seasonal basis because the seasonality of ice core MSA is distorted due to post

Deleted: S3).

Moved (insertion) [1]

209

## 210 3 Results

### 211 3.1 Bromine

212 Ice core measurements of bromine at Summit and Tunu covering the period 1750-2010 are shown in  
213 Fig. 2. Ice core Br levels at each site were stable until ~1830 when they decreased by ~1 nM,  
214 establishing a new baseline that was stable until the early 1900s. Both ice cores also show a Br peak in  
215 the late 20<sup>th</sup> century. The concentration values and the timing of inflections in concentrations were  
216 determined by a 3 step linear regression of the data set. The analysis was performed by simultaneous  
217 linear least squares fitting of 3 straight lines joined by ‘inflection points’ to the data set. The variables  
218 of the fitting procedure were the slopes and intercepts of each line as well as the x-axis locations at  
219 which the total function switched from one linear section to the next (the inflection points). Initial guess  
220 values were supplied for each variable to help the fitting procedure reach reasonable values. A summary  
221 of the regression results can be found in Table S1.

**Deleted:** A summary of the timing of inflections and concentrations  
can be found

222 Sea-salt transport onto the Greenland ice sheet occurs predominantly during winter. Historically the  
223 winter-time sea-salt maximum was believed to be due to increased cyclonic activity over the open  
224 oceans (Fischer and Wagenbach, 1996) though more contemporary studies show that blowing snow  
225 from the surface of sea-ice may be a significant source (Rankin et al., 2002; Xu et al., 2013; Yang et al.,  
226 2008, 2010). At Summit, a winter-time maximum is observed in the most abundant sea salts, Na and Cl  
227 (Fig. 3). Bromine also shows a significant winter-time signal, however the annual maximum appears in  
228 mid-summer - at concentrations ~70% above winter levels (Fig. 3a). Comparison with Br measured in  
229 weekly surface snow samples collected from Summit (from 2007-2013; GEOSummit project) confirms  
230 that this summer signal is real and not a result of post-depositional modification of seasonality of the  
231 bromine signal (Fig. S2). The results from that study confirm that total Br concentrations peak in  
232 summer on the ice sheet closely following the Br cycle observed in the Summit-2010 ice core. In  
233 addition to the comparison with the Geosummit data, in the ice cores studied here there are routinely  
234 more than 10 measurements made within a yearly layer of snow giving confidence to the allocation of  
235 a summer maximum in bromine at Summit. Analysis of the annual cycle of bromine in the Tunu ice  
236 core also shows a summer maximum when averaged over the entire ice core time series but with  
237 significantly larger error than observed at Summit. The timing of this peak suggests a predominant  
238 summer-time deposition of bromine that dwarfs that from winter sea salt sources.

**Deleted:** S1

**Deleted:** source

239 The shape of the annual bromine cycle does change slightly over the course of the Summit record (see



244 Fig. 3). Starting in the early 1900s the annual bromine cycle slowly becomes broader. A slight shift in  
245 the maximum from a solely summer peak in the preindustrial era towards a broad summer-spring peak  
246 by 1970 is observed (Fig. 3 lower plot). Comparison with the sea salt tracer, sodium, which does not  
247 undergo the large temporal shift and broadening of its seasonal cycle shows that this change in bromine  
248 seasonality is not linked to changes in production or transport of sea-salt aerosols or even dating  
249 uncertainties in the ice core but perhaps the introduction of an additional, smaller bromine source in the  
250 spring-time during the industrial era.

251 Both ice cores show a predominantly positive Br enrichment throughout the year (Fig. S3, S4) relative  
252 to both sea salt elements chlorine and sodium. This enrichment reaches a maximum in mid to late  
253 summer at Summit (Fig. 3). We assume that this enrichment reflects Br enrichment in the aerosol  
254 transporting Br to the ice sheet. In a comprehensive review of global aerosol Br measurements, Sander  
255 et al. (2003) concluded that in general, aerosols which showed positive Br enrichment factors were of  
256 sub-micrometer size. These small aerosols can travel further (lifetimes of around 5-10 days) and due to  
257 their larger surface/volume ratio may experience more atmospheric processing than larger aerosols,  
258 resulting in the positive enrichment. However, post-depositional reduction of the bromine concentration  
259 is a possibility during the summer months due to photolytic processes at the snow surface. This may be  
260 the cause of the noisiness of the bromine signal within the lower accumulation, Tunu core. However,  
261 the increased snow accumulation that occurs during the summer months in both central and northern  
262 Greenland (Chen et al., 1997) should act minimise these bromine depleting effects driven by increased  
263 insolation in summer and indeed Weller (2004) has shown that accumulation rates of this size are large  
264 enough to prevent the post-deposition loss of other species such as nitrate and MSA.

265 Both sites also show a (small) positive enrichment of chlorine relative to sodium, which is amplified at  
266 small sodium concentrations. Chlorine containing aerosols are expected to undergo similar chemical  
267 processing to bromine containing aerosols but the enrichment factors of bromine (relative to sodium)  
268 are much larger which is likely due to the high solubility of bromine species such as HBr (Sander et al.,  
269 2003). Alternatively, the chlorine enrichment could be interpreted as a sodium depletion of the aerosols  
270 particularly in those of small diameter where both concentrations are low; this would amplify the  
271 bromine enrichment (relative to sodium) but would not explain the bromine enrichment relative to  
272 chlorine. It is likely that both halogens undergo some degree of enrichment and the sodium undergoes  
273 some depletion in the aerosols though it is difficult to determine this from the data.

274 A summer-time maximum in Br enrichment was also observed by Spolaor (2014) in a short segments  
275 of Antarctic Law Dome ice core as well as two Arctic ice cores. Spolaor et al. believe that the main

Deleted: S2

Deleted: 3). We assume that this enrichment reflects Br enrichment in the aerosol transporting Br to the ice sheet.

Deleted: .

Deleted:

281 source of the inorganic bromine originated from spring-time bromine explosion events above sea ice  
282 and the summer-time maximum could possibly be an indication of lag-time between bromine containing  
283 particles becoming airborne and their deposition. Further investigation is needed to definitively establish  
284 the seasonality of bromine deposition at the poles. However the results of the Arctic ice cores studied  
285 here suggest that the summer maximum in bromine deposition is indeed real.

Deleted: summertime

286 In the Tunu ice core, 11% of the monthly bromine enrichment measurements relative to Na were  
287 negative (less than the Br/Na seawater ratio, Fig. S3) and 12% were negative relative to Cl. It is possible  
288 that the negative enrichment values observed in the Tunu ice core are therefore a result of larger aerosols  
289 (> micrometer) reaching the site due to its proximity to the coast (and thus the likely sea ice aerosol  
290 source region) in comparison to Summit.

Deleted: In the Tunu ice core, 2% of the monthly bromine enrichment measurements (relative to Cl) were negative (less than the Br/Cl seawater ratio, Fig S2). In a comprehensive review of global aerosol Br measurements, Sander (2003) concluded that in general, aerosols which showed positive Br enrichment factors were of sub-micrometer size. These small aerosols can travel further (lifetimes of around 5-10 days) and due to their larger surface/volume ratio may experience more atmospheric processing than larger aerosols, resulting in the positive enrichment.

### 291 3.2 MSA

292 The Summit-2010 MSA record (Fig. 2) replicates that measured by Legrand in 1993 (Legrand et al.,  
293 1997) and extends it an additional 17 years (see Fig. S5). The mean Summit-2010 MSA measurements  
294 over the period 1984-1992 ( $2.0 \pm 0.7$  ( $1\sigma$ ) ppb) also compare well with the results of the sub-annually  
295 sampled Summit snow pit study performed by Jaffrezo et al., (1994);  $2.1 \pm 1.8$  ( $1\sigma$ ) ppb. Both the Legrand  
296 and Jaffrezo studies measured MSA using ion chromatography of discretely sampled snow and ice. The  
297 similarity between the Summit-2010 measurements and the results of these studies demonstrates that  
298 the new, continuous technique is able to achieve a comparable accuracy in MSA measured  
299 concentrations to the traditional, discrete technique. It also demonstrates that negligible amounts of  
300 MSA are being lost by using the continuous melt method.

301 The Tunu measurements represent the first MSA profile at this location. Replicate measurements of the  
302 entire Tunu ice core were performed with the on-line, continuous technique by melting a secondary  
303 stick of ice cut from the original Tunu ice core. The replicate measurements closely followed the original  
304 MSA measurements demonstrating the reproducibility, stability and high precision of the continuous  
305 MSA technique (Fig. S6). The Tunu MSA record was also reproduced using discrete samples collected  
306 from the CFA system (Fig. S7).

307 At Summit, MSA concentrations averaged 48 nM in the late 18<sup>th</sup> century, compared with just 27 nM at  
308 Tunu. From 1878-1930 MSA concentrations at Summit plateaued at 36 nM after which they began to  
309 drop rapidly, at a rate of 0.27 nM/year, reaching 18 nM by 2000 C.E. Large fluctuations in the MSA  
310 record after this time make it difficult to assess the most recent trend in Summit MSA concentrations.  
311 MSA concentrations in the Tunu core showed a similar temporal variability to those in the Summit

Deleted: . The Tunu measurements represent the first MSA profile at this location.

Deleted:

Deleted: .

326 record, and until the mid-20<sup>th</sup> century, were consistently lower in magnitude. MSA concentrations only  
327 began to decline consistently at Tunu after 1984, almost 50 years after the rapid decline observed in the  
328 Summit record. After 2000 C.E., large fluctuations in concentration were again observed making the  
329 modern-day trend in MSA concentration at Tunu difficult to establish.

Deleted: ,

330 Comparison with the total sulfur record (Fig. 4) reveals that during the preindustrial period, MSA  
331 contributes to ~12% and ~ 7% of the total sulfur signal at Summit and Tunu, respectively, compared  
332 with < 2% at the height of industrial period (1970 C.E.) at both sites.

333 The low frequency, preindustrial trend in MSA concentrations seen in these ice core records closely  
334 follows that of bromine; particularly distinct is the decrease in both MSA and bromine at both sites in  
335 the early 1800s (Tables S1 and S2). In the early 1900s, however, both sites show a divergence between  
336 the MSA and Br records—as MSA begins to decline, Br concentrations increase.

337 A dramatic shift in the ‘timing’ of the annual MSA maximum in Summit-2010 ice core is illustrated in  
338 Figs. 3c and S1. The signal shifts gradually and continuously along the length of the the entire Summit-  
339 2010 record from a spring to winter maximum (Fig. S1). This phenomenon has previously been  
340 observed in several Antarctic ice cores and has been attributed to post-depositional migration within the  
341 ice due to salt gradients (Mulvaney et al., 1992; Weller, 2004). At very low accumulation ice core sites  
342 post-depositional loss of MSA (and nitrate) must also be considered. Extrapolation of data collected by  
343 Weller (2004) from a series of East Antarctic ice cores predicts that sites with annual average  
344 accumulations of greater than 105 kg m<sup>-1</sup> yr<sup>-1</sup> (0.105 m yr<sup>-1</sup>) will not show post-depositional loss of  
345 MSA (or nitrate). Both ice cores in this study have sufficient average annual accumulation that post-  
346 depositional loss of MSA (and nitrate) is predicted to be negligible and so is not discussed further.

Deleted: S3

Deleted: S3

### 347 3.3 Acidic Species

348 In winter, with the collapse of the polar vortex, polluted air masses enter the Arctic region as the  
349 phenomenon known as the Arctic haze (Barrie et al., 1981; Li and Barrie, 1993). SO<sub>2</sub> and NO<sub>x</sub> from the  
350 haze are deposited on the ice/snow and oxidised to sulfuric (H<sub>2</sub>SO<sub>4</sub>) and nitric acid (HNO<sub>3</sub>). There are  
351 also natural sources of SO<sub>2</sub> (biomass burning, volcanic eruptions, oceans (Li and Barrie, 1993;  
352 McConnell et al., 2007; Sigl et al., 2013) and NO<sub>x</sub> (microbial activity in soils, biomass burning,  
353 lightning discharges (Vestreng et al., 2009) as well as other snow/ice acidifiers including MSA,  
354 hydrogen chloride and organic acids released from biogenic or biomass burning sources (Pasteris et al.,  
355 2012).

Deleted: ph

Deleted: (

361 The annual cycle for nitrate ( $NO_3^-$ ) is shown in Fig. 3d. Before 1900 C.E. the nitrate shows a seasonal  
 362 maximum in late summer/early fall after which the maximum shifts to late spring/early summer.  
 363 Although there are biological sources of nitrate in the ice core aerosol source regions, in a recent study  
 364 focused on the  $NO_3^-$  and  $\delta^{15}N - NO_3^-$  record in the Summit-2010 ice core, Chellman et al. (2016)  
 365 concluded that the preindustrial (1790-1812 C.E.)  $NO_3^-$  seasonal cycle was driven by biomass burning  
 366 emissions. However, in the modern era (1930-2002 C.E.) oil-burning emissions became the dominant  
 367 source of  $NO_3^-$  in the snow-pack. The change in the dominant  $NO_3^-$  source due to industrialisation is the  
 368 cause of the shift in timing of the seasonal cycle.

369 Total snow acidity was stable at both sites from 1750 through to ~1900 C.E. except for sporadic, short-  
 370 lived spikes due to volcanic eruptions. The average preindustrial acidity was the same at both sites (~1.8  
 371  $\mu M$ ). Both records also show two distinct maxima in acidity centred on 1920 and 1970 C.E. (Fig. 4)  
 372 with Tunu displaying higher acidity than Summit over the entire industrial period. Overlaid with the  
 373 acidity is the total sulfur (S) record for both ice cores. The high correlation between the acidity and S  
 374 records illustrates that the sulfur species are the dominant natural and anthropogenic acidic species in  
 375 the ice cores. The trend in acidity closely follows the global  $SO_2$  emissions with maxima from coal  
 376 (~1920 C.E.) and fossil fuel combustion (~1970 C.E.), respectively (Smith et al., 2011). After 1970 the  
 377 records of acidity and S deviate. This deviation can be attributed to the presence of nitric acid that  
 378 remains at a relatively high concentration in the late 20<sup>th</sup> century whilst sulfur species reduce in  
 379 concentration (Fig. 4).

380  $NO_3^-$  concentrations show no trend during the preindustrial era in either ice core records, averaging  
 381  $1.1(\pm 0.02) \mu M$  and  $1.3(\pm 0.03) \mu M$  for Summit and Tunu, respectively. The higher signal-to-noise ratio  
 382 in the Summit-2010 record reveals a small peak in  $NO_3^-$  concentrations centred on ~1910. The Tunu  
 383 record also shows elevated  $NO_3^-$  concentrations over this period. However the large variability in the  
 384 signal makes it difficult to establish a higher resolution temporal trend. Both records clearly show a  
 385 large increase in  $NO_3^-$  after 1950, peaking in ~1990 and followed by a general decreasing trend with the  
 386 average  $NO_3^-$  levels still double that of preindustrial concentrations:  $2.1 \mu M$  and  $2.3 \mu M$  at Summit and  
 387 Tunu, respectively.

388 The nitrate records from both sites follow the trend in northern hemisphere  $NO_x$  emissions with a peak  
 389 in ~1910 and 1990 C.E.– a result of emissions from increases in both Northern Hemisphere fertilizer  
 390 usage and biomass and fossil fuel combustion (Felix and Elliott, 2013).

Deleted: ph

Deleted: ph

Deleted: )

Deleted: ),

Deleted: ph

Deleted: until 2010 C.E.

397 **3.4 Air mass back trajectories**

398 Air mass back trajectory results demonstrate that air masses reaching the Summit-2010 site between  
399 March and July originate primarily from the South/South-East of the ice core site (Fig. 5a). Previous  
400 back trajectory analyses by Kahl *et al.* (1997) also linked individual spikes in their Summit MSA record  
401 to air masses that had passed over this same region of coast (SE Greenland) within the previous 1-3  
402 days. Similar back trajectories were calculated for Summit-2010 at heights of 500 and 10,000m (Fig.  
403 5a, S8a) illustrating that air masses that travel in the free troposphere and lower troposphere follow  
404 similar back trajectories and likely share the same source regions.

Deleted: 4

405 The results for Tunu indicate that air masses arrive primarily from the west coast of Greenland, passing  
406 over the Baffin Bay area, but there is also significant contribution from both the SE and NE (in May)  
407 coastal areas (Fig. 5b, S8b). Of these two secondary areas it is likely that aerosols transported from the  
408 NE would have a greater influence on the ice core concentrations due to proximity to the ice core site.  
409 Aerosol deposited at Tunu therefore represents a mixture of source regions, but are likely dominated by  
410 the NW Greenland, Baffin Bay coastal region.

Deleted: 6b, S4b

411 **3.5 MSA - Sea Ice correlations**

412 Locations which showed a sea ice concentration (SIC) variability greater than 10% (the average  
413 estimated range of uncertainty in the satellite measurements) and have a significant correlation to MSA  
414 (t-test,  $p < 0.05$ ) are displayed in Fig. 6 and 7. A greater weight must be placed on the post-1979 sea ice  
415 concentration maps (Fig. 6b, Fig. 7b) as these were derived from passive microwave satellite data and,  
416 where available, operational ice chart data. The likely air mass source regions, as defined by the results  
417 of the air mass back trajectories, are indicated by the black bordered regions in Figs. 6 and 7. Within  
418 these areas there is generally a negative correlation between SIC and MSA, particularly in the spring  
419 months and only small patches that show large correlation ( $>0.4$ ). The large areas of positive correlation  
420 along the east coast and in the western Barents Sea are striking, however, these areas are outside of the  
421 defined air mass source region and thus are unlikely to be contributing to the ice core aerosol records.  
422 The positive correlation is likely an artefact of the negative autocorrelation between sea ice conditions  
423 in this region and the SE coast source region (Fig. S9).

Deleted: -

Deleted: -

Deleted: -

Deleted: -

Deleted: S5

424 The effect of the estimated error in dating of the MSA records on the SIC correlation maps is explored  
425 in Fig. S10. By shifting the dating of the MSA records to either extreme of the dating error estimate and  
426 replotting the SIC correlation plots it is clear the error in the dating of the MSA records does not affect  
427 the sign of the correlations displayed on the maps but can have an affect on the magnitude of the

correlation found in different locations. This is likely a result of the peaks in the MSA record being shifted in or out of temporal coherence with peaks in SIC at the different locations.

Over the period 1900-2010 C.E. highly significant correlation (t-test,  $p < 0.001$ ) is found between the annual ice core MSA and the amount of open water in the ice pack (OWIP, representing the area of the marginal sea ice zone, Fig. 6a, Fig. 7a) in these aerosol source areas. For both ice cores the source region OWIP is stable until ~1970, when it begins to decline; a trend followed by the MSA. In the Summit-2010 ice core the highest correlation between annual MSA and monthly OWIP occurs in May ( $r = 0.58$ ,  $p < 0.001$ ) though the following months through to July all show highly significant correlations (July  $r = 0.53$ ,  $p < 0.001$ ). Figs. 3f and S11 demonstrate that this time period (May-July) corresponds to the peak and then rapid decline in the amount of annual OWIP within the Summit-2010 aerosol source area because of the decreasing extent of sea ice. Rapid loss of sea ice reveals areas of biological activity previously capped by the ice allowing surface-atmosphere exchange of DMS, resulting in the seasonal peak in atmospheric MSA correlation with the peak in the area of OWIP.

At Tunu the highest correlation over the 1900-2012 C.E. period is found between annual MSA and annual OWIP ( $r = 0.59$ ,  $p < 0.001$ ), though the July OWIP shows the highest monthly correlation and is also highly significant ( $r = 0.41$ ,  $P < 0.002$ ). Due to the more northerly location of the Tunu aerosol source region, the sea ice pack in this region is generally less fractured and break-up occurs later in the year, with a sharp peak in OWIP occurring in July (Fig. S11). The higher stability of the ice pack throughout the year compared to that in the Summit-2010 source region is the likely reason the Tunu MSA shows highest correlation with the annual average of the OWIP. However, like Summit-2010 the highest monthly OWIP correlation occurs between the annual MSA and the timing of the maximum in annual OWIP (July).

Over the shorter, satellite era (1979–2012 C.E.) again Tunu shows strongest correlation between annual MSA and annual OWIP though at a much lower significance ( $r = 0.32$ ,  $p < 0.05$ ), and the highest monthly correlation occurs in March ( $r = 0.2$ ,  $p < 0.1$ ) albeit with low significance. The significance of the Tunu correlation over this period can be dramatically increased (annual OWIP  $r = 0.54$ ;  $p < 0.001$ , March OWIP  $r = 0.63$ ,  $p < 0.001$ ) if the closer, secondary aerosol source region (NE Greenland,  $80^{\circ}$ – $73^{\circ}$ N,  $20^{\circ}$ – $0^{\circ}$ W) is assumed to also influence the site in equal proportion. March corresponds to the timing of increased insolation and thus the rapid increase in ice algal production (Leu et al., 2015). The shift from a July to March peak in the correlation of OWIP with annual Tunu MSA may be a result of the reduced overall SIE (and thus OWIP) influencing the timing of MSA production. Unfortunately, the post-depositional migration of the MSA signal within the ice cores masks any evidence of true seasonal MSA shifts.

**Deleted:** Over the shorter, satellite era (1979–2010), both the Summit-2010 and Tunu sites show strongest correlation between annual MSA and OWIP in March – when the break-up of the winter sea ice begins ( $r = 0.33$ ,  $p < 0.1$ ;  $r = 0.37$ ,  $p < 0.05$ , Fig. 7b, Fig. 8b). The significance of the Tunu correlation over this period can be dramatically increased ( $r = 0.58$ ;  $p < 0.001$ ), if the closer, secondary source region (NE Greenland) is assumed to also influence the site (not shown).

Summit-2010 also shows a much less significant monthly OWIP correlation with the annual MSA signal over this time period, with the most significant correlation again occurring in March ( $r = 0.4$ ,  $p < 0.02$ ). The greater significance of both the SIC-MSA and OWIP-MSA correlations at both sites over the longer time period is likely a result of the averaging of any MSA production or transport variability as well as the dominance of the low frequency variability of both time series on the overall correlation.

### 3.6 MSA and bromine relationship

In an era where climate is driven by only natural forcings, chemical species that share a common source should show broadly consistent variability. This is evident in the preindustrial section of both ice core records where the relationship between MSA and Br (monitored as Br/MSA) remains constant over the entire period (Fig. 4) despite individual records going through step function changes. Using a 25 year running average on all records, the correlation between MSA and Br over the preindustrial period was calculated as: Summit-2010:  $r = 0.282$  ( $p = 0.0008$ ); Tunu:  $r = 0.298$  ( $p = 0.0004$ ),  $n = 138$ . After ~1930 C.E., relative increases in Br concentrations cause the Br/MSA ratio to increase above the stable preindustrial levels by more than 160%, reaching a peak in ~2000 C.E. at both sites.

Bromine in excess of what is expected from a purely sea ice source (non sea ice bromine,  $nsiBr$ ) was calculated by comparison to the other sea ice proxy, MSA. A linear regression of MSA versus  $Br$  was performed with the preindustrial data (1750-1880 C.E.) to establish the relationship between the two proxies during an era free of anthropogenic forcing (Figure S12a,b). This relationship was then extrapolated into the period after 1880 C.E. in order to estimate the amount of bromine sourced only from sea ice sources during the industrial era. The MSA record was smoothed with a 9<sup>th</sup> order polynomial function before being used in the extrapolation to reduce the noise in the resultant record whilst maintaining the low frequency trends (Figure S12c,d).  $nsiBr$  is thus the difference between the total bromine measured and the calculated, natural sea ice bromine (Figs. 8 and S12e,f); in contrast to  $Br_{exc}$  defined by Spolaor (2016) as the amount of bromine in excess of the Br/Na seawater ratio.

An estimate of the  $nsiBr$  is shown in Fig. 8. By definition,  $nsiBr$  is essentially constant during the preindustrial period, but during the industrial period  $nsiBr$  peaks, reaching a broad maximum between 1980-2000 C.E. of ~3.4nM and 1.9nM at Summit and Tunu, respectively.

## 4 Discussion

The significant correlation between variability of marginal sea ice zone (OWIP) area within the identified source regions and the MSA records suggests that MSA records can be used as a proxy for modern sea ice conditions in these areas. North Atlantic Oscillation (NAO) proxy records developed in

Deleted: ,

Deleted: exBr

Deleted: Br

Deleted: MSA

Deleted: .

Deleted: 5

Deleted: -

Deleted: 264 point Stineman

Deleted: . exBr

Deleted: .

Deleted: amount of bromine measured in excess of what is expected from a purely sea ice source (exBr)

Deleted: exBr

Deleted: exBr

Deleted: 2nM

Deleted: 5nM

Deleted: Assuming that no major changes in atmospheric circulation patterns occurred to change the source regions for the marine aerosols between the preindustrial and industrial periods, our identification of MSA as a sea ice proxy (specifically a marginal sea ice zone proxy) may be valid for time periods both before and after 1850 at each ice core site. One major Northern Hemisphere climate phenomena is the North Atlantic Oscillation (NAO). NAO

529 Greenland ice core records (Appenzeller et al., 1998) suggest that although the northern hemisphere  
530 climate phenomenon has shown variability over the past 200 years, its effect is damped in Northern  
531 Greenland (Appenzeller et al., 1998; Weißbach et al., 2015) so we can assume that no major changes in  
532 atmospheric circulation patterns have occurred to change the source regions for the marine aerosols  
533 between the preindustrial and industrial periods. If this assumption is true, our identification of MSA as  
534 a sea ice proxy (specifically a marginal sea ice zone proxy) may be valid for time periods both before  
535 and after 1850 at each ice core site.

Deleted: NAO

536 The MSA records reveal that after 1820 C.E. a gradual decline in sea ice occurred along the southern  
537 Greenland coast (reflected in the Summit-2010 core) and that this decline in sea ice did not extend  
538 significantly to the most northern Greenland coastline (reflected in the minimal change in Tunu MSA  
539 during this period). It is not unexpected that the Summit-2010 record would show the most dramatic  
540 changes in sea ice since we have demonstrated that the Summit sea ice proxy (MSA) is sourced from  
541 the south-east Greenland coast – an area sensitive to climate changes as it is primarily covered by young,  
542 fragile sea ice. The timing of the sea ice decline is coincident with the end of the Little Ice Age, identified  
543 from  $\delta^{18}\text{O}$  ice core records as spanning the period 1420-1850 C.E. in Greenland (Weißbach et al., 2015).  
544 The dramatic dip in sea ice reflected in both the Tunu MSA and Br records at 1830 C.E. (and also seen  
545 less dramatically in Summit) also appears in the multi-proxy reconstruction of sea ice extent in the  
546 Western Nordic Seas performed by Macias Fauria et. al. (2010). This may be evidence of a 1830 C.E.  
547 sea ice decline event isolated to the east Greenland coast as the ice core records do not replicate the  
548 other dramatic, early 20<sup>th</sup> century fluctuations observed in the latter part of the Western Nordic Seas  
549 reconstruction.

Deleted: .

Deleted: A.D

Deleted: A.D

550 From the ice core records it appears that the greatest decline in Greenland sea ice began in the mid 20<sup>th</sup>  
551 century, dropping to levels that are unprecedented in the last 200 years. This decline is observed along  
552 the entirety of the Greenland coast. Sea ice declined first around the southern coast (from 1930 C.E.,  
553 reflected in Summit-2010) followed 54 years later by the more northern coastline (reflected in the Tunu  
554 record, see infection timings in Table S1). This sea ice decline is coincident with the sustained increase  
555 in greenhouse gases which has been identified as the major climate forcing and driver of increased  
556 global temperatures during the 20<sup>th</sup> century (Mann et al., 1998) and follows the same general trend in  
557 Arctic wide sea ice extent observed by Kinnard (2008).

Deleted: A.D

558 Bromine (more specifically bromine enrichment (Spolaor et al., 2014) and bromine excess (Spolaor et  
559 al., 2016)) has also been suggested as a possible proxy for sea ice conditions, however the timing of the  
560 largest bromine aerosol deposition, in summer, does not coincide with the largest growth or extent of



new sea ice. Sea ice begins to increase only at the end of summer as the fractures in the ice cover are re-laminated and the ice edge begins to advance southward (see Fig. 3f). Fig. S4 compares the record of total bromine and bromine enrichment (calculated relative to sodium,  $\text{enrBr}(\text{Na})$ ) from the Summit-2010 ice core. The only major discrepancies between the two records occur when the total sodium signal has sharp maxima causing dips in the  $\text{enrBr}(\text{Na})$  record in ~1954 and 1990 C.E. and the magnitude of the low frequency variability in  $\text{enrBr}(\text{Na})$  is not as great as in the total bromine record. We are not discounting  $\text{enrBr}(\text{Na})$  as a viable proxy for sea ice conditions, however the use of Na to try and extract the pure sea water component of the Br is complicated by the fact that a lot of Na comes from the sea ice surface as well as from the open ocean. Na itself has been used as a sea ice proxy in several prominent studies (Wais Divide Project Memembers, 2013; Wolff et al., 2003) because, like Br, Na is incorporated into the snow on the surface of the sea ice and can be subsequently blown aloft to produce the atmospheric Na signal seen in the ice core. In addition, the Na concentration is fractionated upon the formation of the ice when mirabolite ( $\text{Na}_2\text{SO}_4$ ) is precipitated out of the brine solution at  $-8^\circ\text{C}$  (Abbott et al., 2012).

So what is the summer-time source of bromine? What is the cause of the increase in spring-time bromine explosion events in the industrial era? (see Fig. 3, lower panel) and why does the bromine record deviate from the sea ice proxy record (MSA) around the same time? Possible sources of bromine and the factors which may effect the resultant bromine deposition flux are discussed below.

#### 4.1 Alternate sources of bromine

##### 4.1.1 Combustion of coal

Bromine is present in coal (Bowen, 1979; Sturges and Harrison, 1986) and coal burning is therefore a potential source of increased bromine deposition on the Greenland ice sheet over the period 1860-1940 (McConnell and Edwards, 2008). McConnell et al. (2008; 2007) demonstrated that pollution from the Northern American coal burning era was deposited all over Greenland leaving as its fingerprint large amounts of black carbon and toxic heavy metals. Sturges (1986) measured the relative concentrations of Br and Pb in particulates emitted from the stacks of coal fired power stations and found a molar ratio (Br:Pb) ranging between 0.36-0.67:1. Figure 8 illustrates that at both Summit and Tunu the  $\text{exPb}$  (lead not from dust sources) preserved in the ice cores over the coal burning era was less than 1nM. This concentration implies that the upper limit to the amount of bromine deposited from coal combustion would be 0.67nM (assuming no loss of bromine from the particulates during transportation). This is an insignificant amount compared to the total Br signal preserved in the ice at this time. Coal combustion

**Deleted:** Bromine has also been suggested as a possible proxy for sea ice conditions, however the timing of the largest bromine aerosol flux, in summer, does not coincide with the largest growth or extent of new sea ice. Sea ice begins to increase only at the end of summer as the fractures in the ice cover are re-laminated and the ice edge begins to advance southward (see Fig. 3f). ... [1]

504 is not the major cause of the elevated industrial Br concentration.

505 **4.1.2 Leaded Gasoline**

506 The largest global, historical, anthropogenic source of bromine is thought to be the combustion of leaded  
507 gasoline. Large quantities of 1,2-dibromoethane (DBE) were added to leaded fuel as a scavenger for Pb  
508 preventing lead oxide deposition by converting it to volatile lead bromide salts as well as  $CH_3Br$  (Berg  
509 et al., 1983; Nriagu, 1990; Oudijk, 2010). In 1925 C.E., gasoline had a Br:Pb molar ratio of 2:1 in a  
510 formulation which is now called “aviation fluid”. The Br:Pb molar ratio was reduced to 1:1 in the 1940s  
511 except in places such as the Soviet Union which continued to use “aviation fluid” for motor gasoline  
512 (Thomas et al., 1997). Although the consumption of leaded gasoline has been well documented,  
513 particularly in North America, the estimates of the emissions of bromine compounds from the  
514 combustion process are still unclear. Estimates of the amount of DBE, that is converted into gaseous  
515  $CH_3Br$  range from 0.1% to 25% (Bertram and Kolowich, 2000) and direct measurements of exhaust  
516 fumes across NW England found a Br:Pb ratio of between (0.65-0.8):1 in the airborne particulates  
517 (Sturges and Harrison, 1986).

518 The ratio of Br:Pb in the gasoline formulae can therefore be used only as an upper limit to predict the  
519 Br:Pb ratio in gasoline combustion aerosols transported to the ice core sites. Figure 8 shows a  
520 comparison between nsiBr and exPb measured in each ice core. Also illustrated is the upper limit of the  
521 amount of bromine expected from gasoline sources assuming the 2:1 Br:Pb ratio for aviation gasoline  
522 over the whole leaded gasoline era. World-wide leaded gasoline emissions were estimated to have  
523 peaked in 1970 C.E. (Thomas et al., 1997)—an assumption that is supported by the observed timing of  
524 the exPb maximum observed in both ice cores. Whilst it is likely that leaded fuel contributed to the  
525 increased bromine observed between 1925 and 1970, it is clear that it was not the only contributor to  
526 the nsiBr record, particularly after 1970 when the nsiBr record continues to rise despite a worldwide  
527 decline in leaded fuel consumption. The disparity between the exPb and nsiBr records suggests the  
528 driving force for the enhanced emission of Br was still active and increasing after 1970.

529 **4.1.3 Seasonal salinity changes**

530 Younger sea ice surfaces such as frost flowers, new and 1<sup>st</sup> year sea ice have a higher salinity and thus  
531 have higher bromine concentrations than older sea ice surfaces (Hunke et al., 2011) . The salinity of sea  
532 ice is at its maximum at the start of the winter season after which surface salinity slowly diminishes due  
533 to gravitational draining (Hunke et al., 2011). As summer approaches, ice continues to undergo  
534 desalination due to melting of surface snow which percolates through the ice (Hunke et al., 2011).

Deleted: , diethyl bromide (DEB)

Deleted: (Oudijk, 2010;Nriagu, 1990;Berg et al., 1983). In 1925

Deleted: (Thomas et al., 1997). Although the

Deleted:

Deleted: B

Deleted: exBr

Deleted: (blue) and just between 1925 and 1940 (green; representing source regions outside the Soviet Union).

Formatted: Not Highlight

Deleted: exBr

Deleted: exBr

Deleted: exBr

Deleted: ing

547 Satellite observations that the BrO flux from the sea ice declines over summer (despite increasing  
548 insolation) is likely due to the combined reduction in young sea ice area and in ice salinity. Ocean  
549 surface salinity decreases in the summer due to the increased meteoric water flux and melting of  
550 desalinated sea ice. Salinity increases are therefore unlikely to be the sole cause of the nsiBr<sub>r</sub> flux  
551 observed in the ice core records and the observed summer maximum in bromine.

Deleted: exBr

#### 552 4.1.4 Organic bromine species

553 Gaseous bromocarbons can be a source of inorganic bromine to the snow pack when they react with  
554 •OH or to a lesser extent with •NO<sub>x</sub> or by photolysis (Kerkweg et al., 2008; WMO, 1995) to form the  
555 less reactive, species *HBr*, *BrNO<sub>3</sub>* and *HOBr*. These species can then be washed out of the atmosphere  
556 and deposited on the snow surface due to their high solubility (Fan and Jacob, 1992; Sander et al., 1999;  
557 Yung et al., 1980).

558 The predominant source of gaseous bromine in the atmosphere is methyl bromide, *CH<sub>3</sub>Br* (WMO,  
559 2002). The major modern sources of *CH<sub>3</sub>Br* are fumigation, biomass burning, leaded fuel combustion,  
560 coastal marshes, wetlands, rapeseed and the oceans (WMO, 2002). The ocean is also a major sink for  
561 *CH<sub>3</sub>Br*, the temperature sensitive dissolution occurring through hydrolysis and chloride ion substitution  
562 to form bromide (WMO, 1995). ~30% of *CH<sub>3</sub>Br* was from industrial emissions at the time of the global  
563 peak in the *CH<sub>3</sub>Br* mixing ratio (1996-1998) (Montzka and Reimann, 2010). The timing of the massive  
564 increases in nsiBr<sub>r</sub> seen at both ice cores sites coincides with the timing of maximum anthropogenic  
565 emissions of *CH<sub>3</sub>Br*. However, the estimated 2.7 ppt increase in global tropospheric *CH<sub>3</sub>Br* above  
566 preindustrial levels equates to only ~ 3.7 ppt (0.05nM) Br incorporated into the snow pack (assuming  
567 100% conversion efficiency of *CH<sub>3</sub>Br* in soluble Br species). This level is far less than the 2-5 nM  
568 increase in nsiBr<sub>r</sub> observed in the ice cores during the industrial period.

Deleted: (Montzka and Reimann, 2010).

Deleted: inorganic bromine

569 Bromoform (*CHBr<sub>3</sub>*) is emitted from vegetation such as marine phytoplankton and seaweed. It has the  
570 largest globe flux of all the bromocarbons (estimated at almost 5 times that of *CH<sub>3</sub>Br* (Kerkweg et al.,  
571 2008). However, it is very short-lived (atmospheric lifetime of ~ 17 days (Ordóñez et al., 2012) and  
572 thus is confined to the marine boundary layer. Inorganic bromine formed from the destruction of *CHBr<sub>3</sub>*  
573 would therefore be representative of only local sources of organic bromine. The biological seasonal  
574 cycle maximises the production of *CHBr<sub>3</sub>* in summer and concentrations are greatly reduced but not  
575 negligible in winter (tidal forcing also influences bromocarbon emission by allowing coastal algae to  
576 dry-out (Kerkweg et al., 2008). The season of Arctic sea ice algae productivity is confined by limitations  
577 in available sunlight and nutrients resulting in a mid-to-late spring maxima – depending upon site  
578 location (Leu et al., 2015) – as is reflected in the seasonality of the MSA record. Direct transport of

Deleted: exBr

583 bromine enriched aerosols from these algal sources to the ice core sites again cannot explain the summer  
584 maximum of bromine observed in the ice. In addition to the incoherence of the seasonality of the  
585 bromine ice core signal, to-date biogenic sources have been considered insignificant sources of bromine  
586 in the Arctic marine boundary layer compared with the inorganic bromine source from sea salts  
587 (Simpson et al., 2007).

**Deleted:** The summer maximum in inorganic bromine at Summit (Fig. 3a) suggests that a biogenic source of bromine is dominant. However to-date biogenic sources have been considered insignificant

**Deleted:** These results suggest that a biogenic system should be reconsidered as a major source of the natural inorganic bromine flux to the polar regions.

## 588 4.2 Cause of the spring-time increase in bromine flux

### 589 4.2.1 Bromine explosion events

590 Spring is the time of ‘bromine explosion’ events above sea ice. Sea salt aerosols passing through these  
591 BrO plumes can become enriched with bromine by adsorbing the gaseous species (Fan and Jacob, 1992;  
592 Langendörfer et al., 1999; Lehrer et al., 1997; Moldanová and Ljungström, 2001; Sander et al., 2003).  
593 Nghiem (2012) showed that these bromine rich air masses can then be elevated above the planetary  
594 boundary layer and transported hundreds of kilometres inland. Increasing the frequency and duration of  
595 the bromine explosion events would therefore likely increase the amount of bromine delivered to the  
596 ice core sites during spring without influencing the total aerosol flux and thus explain the shift in the  
597 bromine seasonal concentrations from a purely summer to a broad spring-summer maxima (Fig. 3).

**Deleted:** (Fan and Jacob, 1992; Langendörfer et al., 1999; Lehrer et al., 1997; Moldanová and Ljungström, 2001; Sander et al., 2003)

**Deleted:** .

598 Spring-time field studies at Ny Ålesund, Svalbard have shown positive correlation between atmospheric  
599 filterable bromine species and elevated levels of sulfate and nitrate (Langendörfer et al., 1999; Lehrer  
700 et al., 1997) suggesting that acidic, anthropogenic pollution may be the driver of the observed increases  
701 in annual bromine enrichment during the industrial period and seasonal shift.

**Deleted:** ph

### 702 4.2.2 Acidity effects on debromination

703 In remote, relatively clean environments such as the Arctic, even small increases in acidity are thought  
704 to affect the cycling of bromine in the snow pack (Finlayson-Pitts, 2003; Pratt et al., 2013; Sander et al.,  
705 1999). In the laboratory, increasing the acidity of frozen (Abbatt et al., 2010) and liquid salt solutions  
706 (Frinak and Abbatt, 2006; George and Anastasio, 2007) increased the yield of gas-phase  $Br_2$  whilst at  
707 the same time increasing the solubility of other bromine species, such as  $HBr$ . The uptake efficiency of  
708  $HBr$  by acidic sulfate aerosols, for example, is estimated at 80% compared to 30% for sea salt aerosols  
709 (Parrella et al., 2012). Interestingly, Abbatt (1995) demonstrated that  $HBr$  is more than 100 times more  
710 soluble in super-cooled sulfuric acid solutions than  $HCl$ . This may explain the cause of bromine  
711 enrichment in the aerosol measured in the ice cores relative to the more abundant chlorine (Fig. S3).

**Deleted:** ph

**Deleted:** ph

**Deleted:** S2

725 The results of both the laboratory and field studies suggest that increasing snow/ice acidity in the Arctic  
726 will likely enhance spring-time bromine explosion events above the sea ice whilst the increase in  
727 solubility allows the termination products of the explosion to be transported away from the sites on the  
728 surface of acidic aerosols. Increasing spring-time bromine aerosol concentrations would increase the  
729 average annual bromine concentrations deposited on the ice sheet and could explain the nsiBr records  
730 observed in both ice cores.

Formatted: Font color: Text 1

Deleted: exBr

Formatted: Font color: Text 1

731 There are also significant periods over which the calculated nsiBr record shows negative values (e.g.  
732 1815-1870 C.E. in Summit-2010 and 1860-1940 C.E. in Tunu). The negative values are a result of the  
733 Total Br being less than that calculated by interpolation from the smoothed MSA record. Though the  
734 sources of Br and MSA are linked – which is what provides the similarities between the general low  
735 frequency trend of the two species, the atmospheric processing, transport and deposition of the two  
736 species may be modified by different variables such as changes in atmospheric acidity, for example.  
737 These variables cause the short term differences between the MSA and Total Br records preserved in  
738 the ice so we believe it is not unreasonable to expect negative values in the calculated non-sea ice Br  
739 record when the MSA and Total Br are close (essentially no nsiBr). The periods of negative nsiBr do  
740 correspond to the timing of increased sulfate concentrations (due to volcanic or industrial activity) and  
741 this could be an indication that the atmospheric sulfate concentrations do have some influence on the  
742 production of either the MSA or Br records.

743 Figure 9 illustrates that of the two dominant acidic species preserved in the ice,  $HNO_3$  (represented by  
744 nitrate) shows the highest correlation to total bromine over sub-decadal time scales at both ice core sites.  
745 Records were detrended with an 11 year running average before comparison to isolate the high  
746 frequency components of each record. The bromine – sulfuric acid (represented by sulfate) correlation  
747 is not significant. This is primarily because there is no bromine response to the dominant volcanic sulfate  
748 spikes throughout the record. The large spikes in sulfate concentrations did not cause a depletion of  
749 bromine preserved in the snowpack (Figure 9). This result might be expected if the increased acidity  
750 caused more bromine to volatilize. These results suggest that  $HNO_3$  is the most influential of the MBL  
751 acidic species in the processing and transport of Br on aerosols in the MBL.

Deleted: ph

#### 752 4.2.3 NO<sub>x</sub> and links to bromine

753 The snow and atmospheric chemistries of bromine and nitrate ( $NO_3^-$ ) are tightly linked.  $NO_3^-$  is one of  
754 the main sources of the •OH radical. The •OH radical can oxidize bromide salts and cause the release  
755 of gas-phase bromine species (Abbatt et al., 2010; Chu and Anastasio, 2005; George and Anastasio,  
756 2007; Jacobi et al., 2014). Morin (2008) observed that the majority of nitrate that is deposited to the

Deleted:

snow surface is of the form  $BrNO_3$  in coastal Arctic boundary layer.  $BrNO_3$  forms by gas-phase reaction of  $BrO$  and  $NO_2$ .  $BrNO_3$  is quickly adsorbed back onto the snow and aerosol surfaces due to its high solubility. The heterogeneous hydrolysis of  $BrNO_3$  to again release bromine species back into the gas-phase has also been observed (Parrella et al., 2012) and can occur both during sunlight hours as well as in the dark (Sander et al., 1999). However, the study of Thomas et al. (2012) into the cycling of  $NO_x$  and bromine species in the snowpack at Summit concluded that the presence of snow  $NO_3^-$  would suppress the emission of  $BrO$  from the snow pack and into the interstitial air.

**Deleted:** in the coastal Arctic boundary layer.

In spring, when the greatest concentrations of  $BrO$  are observed over the sea ice the atmospheric concentrations of  $NO_x$  species is rising. After 1900 C.E. there was, on average, a 60% increase in spring  $NO_3^-$  concentrations observed in Summit-2010 ice core (Fig. 3d) which, as discussed in Sect. 4.2.1, if reflected in the concentration of acidic aerosols landing on the sea ice (specifically  $HNO_3$  concentrations) would enhance the emission of  $BrO$  into the MBL. Satellite imagery shows that bromine in the form of  $BrO$  is confined primarily to the atmosphere above sea ice (Schönhardt et al., 2012; Wagner et al., 2001) but the presence of measurable bromine concentration hundreds of kilometres inland preserved in the ice cores demonstrates that the bromine must be transported inland, just not in the form of  $BrO$ . The reaction of atmospheric  $NO_2$  with  $BrO$  can produce the highly soluble  $BrNO_3$  which will preserve the bromine in the aerosol allowing it to be transported inland. If there are high  $NO_3^-$  concentrations at the deposition site this will aid in fixing the bromine into the snow pack. This is supported by the observation that  $NO_3^-$  snow pack concentrations reach a maximum in summer, coherent with bromine snow pack concentrations even though maximum Br emission from the sea ice occurs in spring. So it appears that  $NO_x$  in its different forms, as  $NO_2$ ,  $NO_3^-$ ,  $HNO_3$  or  $BrNO_3$  is intertwined with Br as it cycles between the gas and condensed phases and as it is transported from sea ice source to deposition site. Elevated levels of  $NO_x$  over the Arctic could thus be the cause of the deviation of the bromine record from the MSA, sea ice proxy record.

**Deleted:**  $NO_x$  are intertwined with Br as it cycles between the gas and condensed phases

**Formatted:** English (US)

The high correlation between the preindustrial (1750-1850 C.E.)  $NO_3^-$  and Br records (Fig. 9) supports this observation of co-transport and sink of Br and  $NO_3^-$  into the snow pack, though the natural sources of each are distinctly different. In the industrial era the low frequency temporal profile of the total bromine and nitrate records differ considerably, particularly at Summit (Fig. S13), apparently questioning the tight relationship observed before 1850. However, the positive correlation between the nitrate and the Br/MSA (Fig. 4) and  $nsiBr$  (Fig. 8) records is striking at both sites. The large relative increase in bromine (compared with MSA) during the era of high  $NO_x$  pollution may point to a non-sea ice source of bromine linked to nitrate emissions or simply an increased spring-time emission and

**Deleted:** The seasonality of the  $NO_3^-$  signal preserved in the ice cores is coherent with Br, showing a summer-time maximum (Fig. 3a,d). The slight shift in timing of the industrial nitrate seasonal maximum towards spring is replicated in the seasonal bromine signal preserved in the ice (Figure 3). The high correlation between the preindustrial (1750-1850)  $NO_3^-$  and Br records (Fig.

**Deleted:** .

**Deleted:** (Fig. 2)

**Deleted:** (Fig. 4)

**Deleted:** dramatically,

305 summer-time deposition of Br from sea ice sources.

306 Bromine and  $NO_x$  species shared a common source in the 20<sup>th</sup> century through the combustion of leaded  
307 gasoline (Sect. 4.1.2). As discussed above, we observe that leaded fuel pollution reaching the Arctic  
308 began to decline after 1970 in-line with reduced global consumption, but the amount of bromine in-  
309 excess of natural sources (nsiBr) continued to increase – following the trends in  $NO_x$  pollution (Fig.  
310 8a). The continued increase in  $NO_x$  despite the decline in leaded fuel combustion is attributed primarily  
311 to biomass burning, soil emissions and unleaded fossil fuel combustion (Lamarque et al., 2013). As the  
312 leaded fuel source of bromine began to decline, organic bromine pollutants continued to increase, as  
313 was discussed in Sect. 4.1.4. This can only account for a small fraction of the observed Br. The  
314 continued correlation between nitrate and nsiBr, despite the decoupling of nitrate and bromine  
315 anthropogenic sources after 1970, suggests that nitrate pollution is likely influencing the processing of  
316 local, natural sources of bromine in the polar MBL, in effect increasing the mobility of the bromine and  
317 thus its flux and preservation in the ice sheet.

Deleted: exBr, Fig. 8

Deleted: 4

Deleted: exBr

Deleted: onto

#### 318 **4.2.4 Consequences of nitrate driven increased bromine mobility in the Arctic**

319 Plumes of BrO emitted from sea ice regions have been linked to mercury deposition events which lead  
320 to an increase in the bioavailability of toxic mercury species in polar waters (Parrella et al., 2012).  
321 Increased spring-time mobilization of bromine from the sea ice induced by anthropogenic nitrate could  
322 therefore increase the frequency and duration of these events and thus the mercury toxicity of the oceans.  
323 Increased atmospheric bromine concentrations would also increase the frequency of ozone depletion  
324 events (Simpson et al., 2007) thereby altering the oxidative chemistry of the polar MBL.  
325 Whilst several studies have begun to explore bromine records from ice cores as a proxy for past sea ice  
326 conditions, the results of this study demonstrate that in an era of massive increases in atmospheric acidity  
327 the natural relationship between bromine and sea ice conditions can become distorted, precluding it  
328 from being an effective modern-day Arctic sea ice proxy.

## 330 **5 Conclusion**

331 In this study we have shown that high resolution MSA measurements preserved in ice cores can be used  
332 as a proxy for sea ice conditions (specifically the size of the marginal sea ice zone) along specific  
333 sections of the Greenland coast. The MSA records show that sea ice began to decline at the end of the  
334 LIA and again, more dramatically during the Industrial period. Also, unsurprisingly, the changes in sea  
335 ice conditions in the northern sites have been less dramatic than along the southern coastline.

340 Comparison between the 260 year records of bromine and MSA presented in this study allow us to show  
341 that in the preindustrial era bromine concentrations preserved in the Greenland ice sheet are also likely  
342 linked to the local sea ice conditions. With the decline of sea ice in the modern era and the dramatic  
343 increase in acidic pollutants reaching the Arctic the sea ice-bromine connection is distorted, precluding  
344 it from being an effective, direct sea ice proxy during the industrial era. The introduction of *NO<sub>x</sub>*  
345 pollution in particular, into the clean Arctic environment promotes mobilization of bromine from the  
346 sea ice, which in turn increases the bromine enrichment of the sea salt aerosols, forcing more bromine  
347 inland (particularly in spring) than would occur naturally. Nitrate has also been linked with the  
348 mechanism for preservation of bromine in the snowpack. The summer-time maximum of nitrate may  
349 therefore be responsible for the observed summer-time bromine maximum preserved in the ice cores.  
350 Whilst Northern Hemisphere pollution may prevent bromine from being an effective modern-day sea  
351 ice proxy in the Arctic, in Antarctica the anthropogenic flux of nitrate species is thought to be small in  
352 comparison with natural sources (Wolff, 2013), leaving room for the possibility that bromine may still  
353 be an effective proxy for local Antarctic sea ice conditions.

Deleted: NO<sub>x</sub>



357 **Author contribution**

358 Manuscript written and data analysis performed by O.J.M with expert editing by E.S.. Ice cores supplied  
359 by J.R.M.. Tunu ice core was collected and processed by O.J.M, J.R.M., N.J.C, M.S., R.H.R. under the  
360 leadership of Beth Bergeron. Ice cores dated by M.S., J.R.M.. ICP-MS and CFA measurements  
361 performed by O.J.M, J.R.M., N.J.C., L.L, D.P., M.S.. MSA measurements designed and performed by  
362 M.G., E.S.

363

364 **Acknowledgements**

365 This research was funded by the National Science Foundation; grant numbers 1023672 and 1204176.

366

## References

- Abbatt, J., Oldridge, N., Symington, a, Chukalovskiy, V., McWhinney, R. D., Sjostedt, S. and Cox, R. a: Release of gas-phase halogens by photolytic generation of OH in frozen halide-nitrate solutions: an active halogen formation mechanism?, *J. Phys. Chem. A*, 114(23), 6527–33, doi:10.1021/jp102072t, 2010.
- Abbatt, J. P. D.: Interactions of HBr, HCl, and HOBr With Supercooled Sulfuric- Acid-Solutions of Stratospheric Composition, *J. Geophys. Res.*, 100(D7), 14009–14017, 1995.
- Abbatt, J. P. D., Thomas, J. L., Abrahamsson, K., Boxe, C., Granfors, A., Jones, A. E., King, M. D., Saiz-Lopez, A., Shepson, P. B., Sodeau, J., Toohey, D. W., Toubin, C., von Glasow, R., Wren, S. N. and Yang, X.: Halogen activation via interactions with environmental ice and snow in the polar lower troposphere and other regions, *Atmos. Chem. Phys.*, 12(14), 6237–6271, doi:10.5194/acp-12-6237-2012, 2012.
- Abram, N. J., Wolff, E. W. and Curran, M. A. J.: A review of sea ice proxy information from polar ice cores, *Quat. Sci. Rev.*, 79, 168–183, doi:10.1016/j.quascirev.2013.01.011, 2013.
- Appenzeller, C., Schwander, J., Sommer, S. and Stocker, T. F.: The North Atlantic Oscillation and its imprint on precipitation and ice accumulation in Greenland, *Geophys. Res. Lett.*, 25(11), 1939, doi:10.1029/98GL01227, 1998.
- Barrie, L. A., Hoff, R. M. and Daggupaty, S. M.: The influence of mid-latitudinal pollution sources on haze in the Canadian arctic, *Atmos. Environ.*, 15(8), 1407–1419, doi:10.1016/0004-6981(81)90347-4, 1981.
- Berg, W. W., Sperry, P. D., Rahn, K. A. and Gladney, E. S.: Atmospheric Bromine in the Arctic, *J. Geophys. Res.*, 88, 6719–6736, doi:10.1029/JC088iC11p06719, 1983.
- Bertram, F. J. and Kolowich, J. B.: A study of methyl bromide emissions from automobiles burning leaded gasoline using standardized vehicle testing procedures, *Geophys. Res. Lett.*, 27(9), 1423–1426, doi:10.1029/1999GL011008, 2000.
- Bowen, H. J. M.: *Environmental chemistry of the elements* / H. J. M. Bowen, Academic Press, London ; New York., 1979.
- Chellman, N. J., Hastings, M. G. and McConnell, J. R.: Increased nitrate and decreased  $\delta^{15}\text{N}-\text{NO}_3^-$  in the Greenland Arctic after 1940 attributed to North American oil burning, *Cryosph. Discuss.*, 1–22, doi:10.5194/tc-2016-163, 2016.

397 Chen, Q. S., Bromwich, D. H. and Bai, L.: Precipitation over Greenland retrieved by a dynamic method  
 398 and its relation to cyclonic activity, *J. Clim.*, 10(5), 839–870, 1997.

399 Chu, L. and Anastasio, C.: Formation of hydroxyl radical from the photolysis of frozen hydrogen  
 400 peroxide, *J. Phys. Chem. A*, 109(28), 6264–6271, doi:10.1021/jp051415f, 2005.

401 Curran, M. A. J. and Jones, G. B.: Dimethyl sulfide in the Southern Ocean: Seasonality and flux, *J.*  
 402 *Geophys. Res.*, 105(D16), 20451, doi:10.1029/2000JD900176, 2000.

403 Curran, M. A. J., van Ommen, T. D., Morgan, V. I., Phillips, K. L. and Palmer, A. S.: Ice core evidence  
 404 for Antarctic sea ice decline since the 1950s., *Science*, 302(5648), 1203–1206,  
 405 doi:10.1126/science.1087888, 2003.

406 Draxler, R. R. and Hess, G. D.: An Overview of the HYSPLIT\_4 Modelling System for Trajectories,  
 407 Dispersion, and Deposition., *Aust. Meteorol. Mag.*, 47(June 1997), 295–308, 1998.

408 Fan, S.-M. and Jacob, D. J.: Surface ozone depletion in Arctic spring sustained by bromine reactions on  
 409 aerosols, *Nature*, 359(6395), 522–524, doi:10.1038/359522a0, 1992.

410 Felix, J. D. and Elliott, E. M.: The agricultural history of human-nitrogen interactions as recorded in ice  
 411 core  $\delta^{15}\text{N-NO}_3^-$ , *Geophys. Res. Lett.*, 40(8), 1642–1646, doi:10.1002/grl.50209, 2013.

412 Finlayson-Pitts, B. J.: The Tropospheric Chemistry of Sea Salt: A Molecular-Level View of the  
 413 Chemistry of NaCl and NaBr, *Chem. Rev.*, 103(12), 4801–4822, doi:10.1021/cr020653t, 2003.

414 Fischer, H. and Wagenbach, D.: Large-scale spatial trends in recent firn chemistry along an east-west  
 415 transect through central Greenland, *Atmos. Environ.*, 30(19), 3227–3238, doi:10.1016/1352-  
 416 2310(96)00092-1, 1996.

417 Frinak, E. K. and Abbatt, J. P. D.: Br<sub>2</sub> production from the heterogeneous reaction of gas-phase OH  
 418 with aqueous salt solutions: Impacts of acidity, halide concentration, and organic surfactants., *J. Phys.*  
 419 *Chem. A*, 110(35), 10456–64, doi:10.1021/jp063165o, 2006.

420 George, I. J. and Anastasio, C.: Release of gaseous bromine from the photolysis of nitrate and hydrogen  
 421 peroxide in simulated sea-salt solutions, *Atmos. Environ.*, 41(3), 543–553,  
 422 doi:10.1016/j.atmosenv.2006.08.022, 2007.

423 Hunke, E. C., Notz, D., Turner, A. K. and Vancoppenolle, M.: The multiphase physics of sea ice: a  
 424 review for model developers, *Cryosph.*, 5(4), 989–1009, doi:10.5194/tc-5-989-2011, 2011.

425 Jacobi, H. W., Kleffmann, J., Villena, G., Wiesen, P., King, M., France, J., Anastasio, C. and Staebler,  
 426 R.: Role of nitrite in the photochemical formation of radicals in the snow, *Environ. Sci. Technol.*, 48(1),

165–172, doi:10.1021/es404002c, 2014.

Kahl, J. D. W., Martinez, D. A., Kuhns, H., Davidson, C. I., Jafferezo, J. L. and Harris, J. M.: Air mass trajectories to Summit, Greenland : A 44-year climatology and some episodic events, *J. Geophys. Res. Ocean.*, 102(C12), 26861–26875, 1997.

Kerkweg, A., Jöckel, P., Warwick, N., Gebhardt, S., Brenninkmeijer, C. a. M. and Lelieveld, J.: Consistent simulation of bromine chemistry from the marine boundary layer to the stratosphere – Part 2 : Bromocarbons, *Atmos. Chem. Phys. Discuss.*, 8(3), 9477–9530, doi:10.5194/acpd-8-9477-2008, 2008.

Kinnard, C., Zdanowicz, C. M., Koerner, R. M. and Fisher, D. A.: A changing Arctic seasonal ice zone: Observations from 1870–2003 and possible oceanographic consequences, *Geophys. Res. Lett.*, 35(2), 2–6, doi:10.1029/2007GL032507, 2008.

Lamarque, J.-F., Dentener, F., McConnell, J., Ro, C.-U., Shaw, M., Vet, R., Bergmann, D., Cameron-Smith, P., Dalsoren, S., Doherty, R., Faluvegi, G., Ghan, S. J., Josse, B., Lee, Y. H., MacKenzie, I. A., Plummer, D., Shindell, D. T., Skeie, R. B., Stevenson, D. S., Strode, S., Zeng, G., Curran, M., Dahl-Jensen, D., Das, S., Fritzsche, D. and Nolan, M.: Multi-model mean nitrogen and sulfur deposition from the Atmospheric Chemistry and Climate Model Intercomparison Project (ACCMIP): evaluation of historical and projected future changes, *Atmos. Chem. Phys.*, 13(16), 7997–8018, doi:10.5194/acp-13-7997-2013, 2013.

Langendörfer, U., Lehrer, E., Wagenbach, D. and Platt, U.: Observation of filterable bromine variabilities during Arctic tropospheric ozone depletion events in high (1 hour) time resolution, in *Journal of Atmospheric Chemistry*, vol. 34, pp. 39–54., 1999.

Legrand, M., Hammer, C., De Angelis, M., Savarino, J., Delmas, R., Clausen, H. and Johnsen, S. J.: Sulfur-containing species (methanesulfonate and SO<sub>4</sub>) over the last climatic cycle in the Greenland Ice Core Project (central Greenland) ice core, *J. Geophys. Res.*, 102(C12), 26663, doi:10.1029/97JC01436, 1997.

Lehrer, E., Wagenbach, D. and Platt, U.: Aerosol chemical composition during tropospheric ozone depletion at Ny Ålesund/Svalbard, *Tellus B*, 49(5), doi:10.3402/tellusb.v49i5.15987, 1997.

Leu, E., Mundy, C. J., Assmy, P., Campbell, K., Gabrielsen, T. M., Gosselin, M., Juul-Pedersen, T. and Gradinger, R.: Arctic spring awakening - Steering principles behind the phenology of vernal ice algal blooms, *Prog. Oceanogr.*, 139, 151–170, doi:10.1016/j.pocean.2015.07.012, 2015.

Li, S.-M. and Barrie, L. A.: Biogenic sulfur aerosol in the Arctic troposphere: 1. Contributions to total

sulfate, *J. Geophys. Res.*, 98(D11), 20613, doi:10.1029/93JD02234, 1993.

Macias Fauria, M., Grinsted, A., Helama, S., Moore, J., Timonen, M., Martma, T., Isaksson, E. and Eronen, M.: Unprecedented low twentieth century winter sea ice extent in the Western Nordic Seas since A.D. 1200, *Clim. Dyn.*, 34(6), 781–795, doi:10.1007/s00382-009-0610-z, 2010.

Mann, M. E., Bradley, R. S. and Hughes, M. K.: Global-scale temperature patterns and climate forcing over the past six centuries, *Nature*, 392(6678), 779–787, doi:10.1038/33859, 1998.

McConnell, J. R. and Edwards, R.: Coal burning leaves toxic heavy metal legacy in the Arctic., *Proc. Natl. Acad. Sci. U. S. A.*, 105(34), 12140–12144, doi:10.1073/pnas.0803564105, 2008.

McConnell, J. R., Lamorey, G. W., Lambert, S. W. and Taylor, K. C.: Continuous ice-core chemical analyses using inductively coupled plasma mass spectrometry., *Environ. Sci. Technol.*, 36(775), 7–11, doi:10.1021/es011088z, 2002.

McConnell, J. R., Edwards, R., Kok, G. L., Flanner, M. G., Zender, C. S., Saltzman, E. S., Banta, J. R., Pasteris, D. R., Carter, M. M. and Kahl, J. D. W.: 20th-Century Industrial Black Carbon Emissions Altered Arctic Climate Forcing, *Science* (80-. ), 317(5843), 1381–1384, doi:10.1126/science.1144856, 2007.

Millero, F. J.: The Physical Chemistry of Seawater, *Annu. Rev. Earth Planet. Sci.*, 2(1), 101–150, doi:10.1146/annurev.ea.02.050174.000533, 1974.

Moldanová, J. and Ljungström, E.: Sea-salt aerosol chemistry in coastal areas: A model study, *J. Geophys. Res.*, 106, 1271, doi:10.1029/2000JD900462, 2001.

Montzka, S. and Reimann, S.: Scientific Assessment of Ozone Depletion 2010: Scientific Summary Chapter 1 Ozone-Depleting Substances (ODSs) and Related Chemicals. [online] Available from: <http://www.esrl.noaa.gov/csd/assessments/ozone/2010/summary/ch1.html> (Accessed 23 December 2015), 2010.

Morin, S., Savarino, J., Frey, M. M., Yan, N., Bekki, S., Bottenheim, J. and Martins, J. M. F.: Tracing the origin and fate of NO<sub>x</sub> in the Arctic atmosphere using stable isotopes in nitrate., *Science*, 322(5902), 730–2, doi:10.1126/science.1161910, 2008.

Mulvaney, R., Pasteur, E. C., Peel, D. A., Saltzman, E. S. and Whung, P.-Y.: The ratio of MSA to non-sea-salt sulphate in Antarctic Peninsula ice cores, *Tellus B*, 44(4), doi:10.3402/tellusb.v44i4.15457, 1992.

Nghiem, S. V., Rigor, I. G., Richter, A., Burrows, J. P., Shepson, P. B., Bottenheim, J., Barber, D. G.,

988 Steffen, A., Latonas, J., Wang, F., Stern, G., Clemente-Colón, P., Martin, S., Hall, D. K., Kaleschke, L.,  
 989 Tackett, P., Neumann, G. and Asplin, M. G.: Field and satellite observations of the formation and  
 990 distribution of Arctic atmospheric bromine above a rejuvenated sea ice cover, *J. Geophys. Res. Atmos.*,  
 991 117(D17), n/a–n/a, doi:10.1029/2011JD016268, 2012.

992 Nriagu, J. O.: The rise and fall of leaded gasoline, *Sci. Total Environ.*, 92, 13–28, 1990.

993 O'Dwyer, J., Isaksson, E., Vinje, T., Jauhiainen, T., Moore, J., Pohjola, V., Vaikmae, R. and van de  
 994 Wal, R. S. W.: Methanesulfonic acid in a Svalbard ice core as an indicator of ocean climate, *Geophys.*  
 995 *Res. Lett.*, 27(8), 1159–1162, doi:10.1029/1999GL011106, 2000.

996 Ordóñez, C., Lamarque, J.-F., Tilmes, S., Kinnison, D. E., Atlas, E. L., Blake, D. R., Sousa Santos, G.,  
 997 Brasseur, G. and Saiz-Lopez, A.: Bromine and iodine chemistry in a global chemistry-climate model:  
 998 description and evaluation of very short-lived oceanic sources, *Atmos. Chem. Phys.*, 12(3), 1423–1447,  
 999 doi:10.5194/acp-12-1423-2012, 2012.

1000 Oudijk, G.: The Rise and Fall of Organometallic Additives in Automotive Gasoline, *Environ. Forensics*,  
 1001 11(933126918), 17–49, doi:10.1080/15275920903346794, 2010.

1002 Parrella, J. P., Jacob, D. J., Liang, Q., Zhang, Y., Mickley, L. J., Miller, B., Evans, M. J., Yang, X., Pyle,  
 1003 J. A., Theys, N. and Van Roozendaal, M.: Tropospheric bromine chemistry: implications for present  
 1004 and pre-industrial ozone and mercury, *Atmos. Chem. Phys.*, 12(15), 6723–6740, doi:10.5194/acp-12-  
 1005 6723-2012, 2012.

1006 Pasteris, D. R., McConnell, J. R. and Edwards, R.: High-resolution, continuous method for measurement  
 1007 of acidity in ice cores, *Environ. Sci. Technol.*, 46, 1659–1666, doi:10.1021/es202668n, 2012.

1008 Pratt, K. A., Custard, K. D., Shepson, P. B., Douglas, T. A., Pöhler, D., General, S., Zielcke, J., Simpson,  
 1009 W. R., Platt, U., Tanner, D. J., Gregory Huey, L., Carlsen, M. and Stirm, B. H.: Photochemical  
 1010 production of molecular bromine in Arctic surface snowpacks, *Nat. Geosci.*, 6(5), 351–356,  
 1011 doi:10.1038/ngeo1779, 2013.

1012 Rankin, A. M., Wolff, E. W. and Martin, S.: Frost flowers: Implications for tropospheric chemistry and  
 1013 ice core interpretation, *J. Geophys. Res. Atmos.*, 107(D23), 4683, doi:10.1029/2002JD002492, 2002.

1014 Rayner, N. A.: Global analyses of sea surface temperature, sea ice, and night marine air temperature  
 1015 since the late nineteenth century, *J. Geophys. Res.*, 108(D14), 4407, doi:10.1029/2002JD002670, 2003.

1016 Röthlisberger, R., Bigler, M., Hutterli, M., Sommer, S., Stauffer, B., Junghans, H. G. and Wagenbach,  
 1017 D.: Technique for continuous high-resolution analysis of trace substances in firn and ice cores, *Environ.*

Sci. Technol., 34(2), 338–342, doi:10.1021/es9907055, 2000.

Röthlisberger, R., Mulvaney, R., Wolff, E. W., Hutterli, M. a., Bigler, M., Sommer, S. and Jouzel, J.: Dust and sea salt variability in central East Antarctica (Dome C) over the last 45 kyrs and its implications for southern high-latitude climate, *Geophys. Res. Lett.*, 29(20), 1–4, doi:10.1029/2003GL016936, 2002.

Saltzman, E. S., Dioumaeva, I. and Finley, B. D.: Glacial/interglacial variations in methanesulfonate (MSA) in the Siple Dome ice core, West Antarctica, *Geophys. Res. Lett.*, 33(11), 1–4, doi:10.1029/2005GL025629, 2006.

Sander, R., Rudich, Y., von Glasow, R. and Crutzen, P. J.: The role of BrNO<sub>3</sub> in marine tropospheric chemistry: A model study, *Geophys. Res. Lett.*, 26(18), 2857–2860, doi:10.1029/1999GL900478, 1999.

Sander, R., Keene, W. C., Pszenny, A. A. P., Arimoto, R., Ayers, G. P., Baboukas, E., Cainey, J. M., Crutzen, P. J., Duce, R. A., Hönninger, G., Huebert, B. J., Maenhaut, W., Mihalopoulos, N., Turekian, V. C. and Van Dingenen, R.: Inorganic bromine in the marine boundary layer: a critical review, *Atmos. Chem. Phys.*, 3, 1301–1336, doi:10.5194/acp-3-1301-2003, 2003.

Schönhardt, A., Begoin, M., Richter, A., Wittrock, F., Kaleschke, L., Gómez Martín, J. C. and Burrows, J. P.: Simultaneous satellite observations of IO and BrO over Antarctica, *Atmos. Chem. Phys.*, 12(14), 6565–6580, doi:10.5194/acp-12-6565-2012, 2012.

Sharma, S., Chan, E., Ishizawa, M., Toom-Sauntry, D., Gong, S. L., Li, S. M., Tarasick, D. W., Leaitch, W. R., Norman, a., Quinn, P. K., Bates, T. S., Lefvasseur, M., Barrie, L. a. and Maenhaut, W.: Influence of transport and ocean ice extent on biogenic aerosol sulfur in the Arctic atmosphere, *J. Geophys. Res. Atmos.*, 117(12), n/a–n/a, doi:10.1029/2011JD017074, 2012.

Sigl, M., McConnell, J. R., Layman, L., Maselli, O. J., McGwire, K., Pasteris, D., Dahl-Jensen, D., Steffensen, J. P., Vinther, B., Edwards, R., Mulvaney, R. and Kipfstuhl, S.: A new bipolar ice core record of volcanism from WAIS Divide and NEEM and implications for climate forcing of the last 2000 years, *J. Geophys. Res. Atmos.*, 118(3), 1151–1169, doi:10.1029/2012JD018603, 2013.

Sigl, M., Winstrup, M., McConnell, J. R., Welten, K. C., Plunkett, G., Ludlow, F., Büntgen, U., Caffee, M., Chellman, N., Dahl-Jensen, D., Fischer, H., Kipfstuhl, S., Kostick, C., Maselli, O. J., Mekhaldi, F., Mulvaney, R., Muscheler, R., Pasteris, D. R., Pilcher, J. R., Salzer, M., Schüpbach, S., Steffensen, J. P., Vinther, B. M. and Woodruff, T. E.: Timing and climate forcing of volcanic eruptions for the past 2,500 years, *Nature*, 523(7562), 543–9, doi:10.1038/nature14565, 2015.

Simpson, W. R., von Glasow, R., Riedel, K., Anderson, P., Ariya, P., Bottenheim, J., Burrows, J., Carpenter, L. J., Friess, U., Goodsite, M. E., Heard, D., Hutterli, M., Jacobi, H.-W., Kaleschke, L., Neff,

Deleted: a. a

Deleted: a

Deleted: Maenhaut

Deleted: . Discuss

Deleted: d

Deleted: 2963

055 B., Plane, J., Platt, U., Richter, a., Roscoe, H., Sander, R., Shepson, P., Sodeau, J., Steffen, a., Wagner,  
 056 T. and Wolff, E.: Halogens and their role in polar boundary-layer ozone depletion, , 4375–4418,  
 057 doi:10.5194/acpd-7-4285-2007, 2007.

058 Sjostedt, S. J., Huey, L. G., Tanner, D. J., Peischl, J., Chen, G., Dibb, J. E., Lefer, B., Hutterli, M. a.,  
 059 Beyersdorf, a. J., Blake, N. J., Blake, D. R., Sueper, D., Ryerson, T., Burkhardt, J. and Stohl, a.:  
 060 Observations of hydroxyl and the sum of peroxy radicals at Summit, Greenland during summer 2003,  
 061 Atmos. Environ., 41(24), 5122–5137, doi:10.1016/j.atmosenv.2006.06.065, 2007.

062 Smith, S. J., van Aardenne, J., Klimont, Z., Andres, R. J., Volke, A. and Delgado Arias, S.:  
 063 Anthropogenic sulfur dioxide emissions: 1850–2005, Atmos. Chem. Phys., 11(3), 1101–1116,  
 064 doi:10.5194/acp-11-1101-2011, 2011.

065 Spolaor, A., Vallelonga, P., Plane, J. M. C., Kehrwald, N., Gabrieli, J., Varin, C., Turetta, C., Cozzi, G.,  
 066 Kumar, R., Boutron, C. and Barbante, C.: Halogen species record Antarctic sea ice extent over glacial-  
 067 interglacial periods, Atmos. Chem. Phys., 13, 6623–6635, doi:10.5194/acp-13-6623-2013, 2013a.

068 Spolaor, A., Gabrieli, J., Martma, T., Kohler, J., Björkman, M. B., Isaksson, E., Varin, C., Vallelonga,  
 069 P., Plane, J. M. C. and Barbante, C.: Sea ice dynamics influence halogen deposition to Svalbard,  
 070 Cryosph., 7(5), 1645–1658, doi:10.5194/tc-7-1645-2013, 2013b.

071 Spolaor, A., Vallelonga, P., Gabrieli, J., Martma, T., Björkman, M. P., Isaksson, E., Cozzi, G., Turetta,  
 072 C., Kjær, H. A., Curran, M. A. J., Moy, A. D., Schönhardt, A., Blechschmidt, A.-M., Burrows, J. P.,  
 073 Plane, J. M. C. and Barbante, C.: Seasonality of halogen deposition in polar snow and ice, Atmos. Chem.  
 074 Phys., 14(18), 9613–9622, doi:10.5194/acp-14-9613-2014, 2014.

075 Spolaor, A., Opel, T., McConnell, J. R., Maselli, O. J., Spreen, G., Varin, C., Kirchgeorg, T., Fritzsche,  
 076 D., Saiz-Lopez, A. and Vallelonga, P.: Halogen-based reconstruction of Russian Arctic sea ice area  
 077 from the Akademii Nauk ice core (Severnaya Zemlya), Cryosph., 10, 245–256, doi:10.5194/tcd-9-4407-  
 078 2015, 2016.

079 Sturges, W. T. and Harrison, R. M.: Bromine:Lead ratios in airborne particles from urban and rural sites,  
 080 Atmos. Environ., 20(3), 577–588, doi:10.1016/0004-6981(86)90101-0, 1986.

081 Thomas, J. L., Dibb, J. E., Huey, L. G., Liao, J., Tanner, D., Lefer, B., von Glasow, R. and Stutz, J.:  
 082 Modeling chemistry in and above snow at Summit, Greenland – Part 2: Impact of snowpack chemistry  
 083 on the oxidation capacity of the boundary layer, Atmos. Chem. Phys., 12(14), 6537–6554,  
 084 doi:10.5194/acp-12-6537-2012, 2012.

085 Thomas, V. M., Bedford, J. A. and Cicerone, R. J.: Bromine emissions from leaded gasoline, Geophys.



Res. Lett., 24(11), 1371–1374, doi:10.1029/97GL01243, 1997.

Vestreng, V., Ntziachristos, L., Semb, A., Reis, S., Isaksen, I. S. A. and Tarrasón, L.: Evolution of NO<sub>x</sub> emissions in Europe with focus on road transport control measures, Atmos. Chem. Phys., 9(4), 1503–1520, doi:10.5194/acp-9-1503-2009, 2009.

Wagner, T., Leue, C., Wenig, M., Pfeilsticker, K. and Platt, U.: Spatial and temporal distribution of enhanced boundary layer BrO concentrations measured by the GOME instrument aboard ERS-2, J. Geophys. Res., 106(D20), 24225, doi:10.1029/2000JD000201, 2001.

[Wais Divide Project Memembers: Onset of deglacial warming in West Antarctica driven by local orbital forcing., Nature, 500\(7463\), 440–4, doi:10.1038/nature12376, 2013.](#)

Walsh, J. E.: A data set on Northern Hemisphere sea ice extent, Natl. Snow Ice Data Cent., 49–51, 1978.

Weißbach, S., Wegner, A., Opel, T., Oerter, H., Vinther, B. M. and Kipfstuhl, S.: Spatial and temporal oxygen isotope variability in northern Greenland - implications for a new climate record over the past millennium, Clim. Past Discuss., 11(3), 2341–2388, doi:10.5194/cpd-11-2341-2015, 2015.

Weller, R.: Postdepositional losses of methane sulfonate, nitrate, and chloride at the European Project for Ice Coring in Antarctica deep-drilling site in Dronning Maud Land, Antarctica, J. Geophys. Res., 109(D7), 1–9, doi:10.1029/2003JD004189, 2004.

WMO: Scientific Assessment of Ozone Depletion: 1994. Chapter 10: Methyl Bromide, Geneva., 1995.

WMO: Scientific Assessment of Ozone Depletion: 2002. Chapter 1: Controlled Substances and Other Source Gases., 2002.

Wolff, E. W.: Ice sheets and nitrogen, Philos. Trans. R. Soc. Lond. B. Biol. Sci., 368, doi:10.1098/rstb.2013.0127, 2013.

Wolff, E. W., Rankin, A. M. and Röthlisberger, R.: An ice core indicator of Antarctic sea ice production?, Geophys. Res. Lett., 30(22), 2–5, doi:10.1029/2003GL018454, 2003.

Xu, L., Russell, L. M., Somerville, R. C. J. and Quinn, P. K.: Frost flower aerosol effects on Arctic wintertime longwave cloud radiative forcing, J. Geophys. Res. Atmos., 118(23), 13282–13291, doi:10.1002/2013JD020554, 2013.

Yang, X., Pyle, J. A. and Cox, R. A.: Sea salt aerosol production and bromine release: Role of snow on sea ice, Geophys. Res. Lett., 35(16), 1–5, doi:10.1029/2008GL034536, 2008.

Yang, X., Pyle, J. A., Cox, R. A., Theys, N. and Van Roozendaal, M.: Snow-sourced bromine and its

115 implications for polar tropospheric ozone, *Atmos. Chem. Phys.*, 10(16), 7763–7773, doi:10.5194/acp-  
116 10-7763-2010, 2010.

117 Yung, Y. L., Pinto, J. P., Watson, R. T. and Sander, S. P.: Atmospheric Bromine and Ozone  
118 Perturbations in the Lower Stratosphere, *J. Atmos. Sci.*, 37(2), 339–353, doi:10.1175/1520-  
119 0469(1980)037<0339:ABAOPI>2.0.CO;2, 1980.

120  
121

122

123

124

125

126

127

128

129

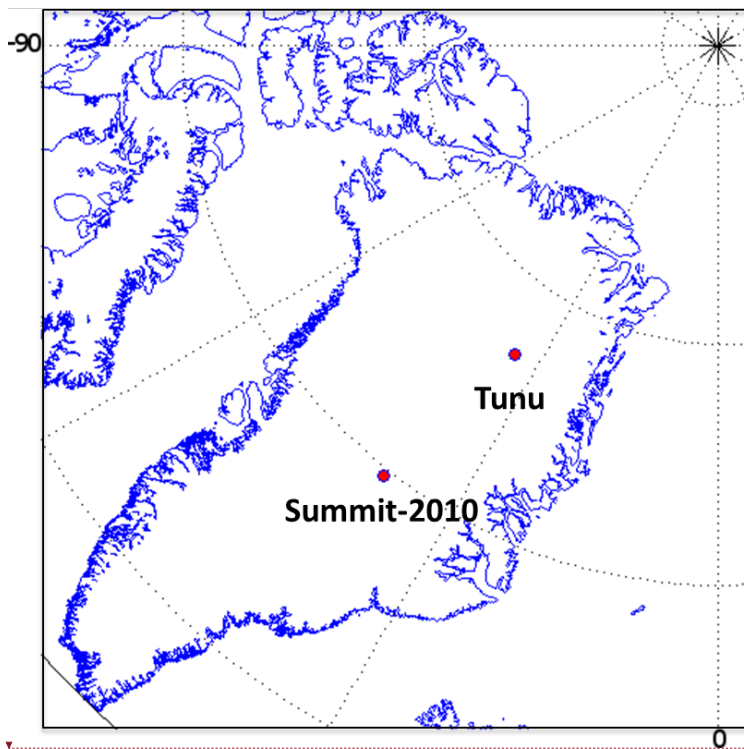


**Figure 1.** Locations of ice cores used in this study. Summit-2010: (72°20'N 38°17'24"W), Tunu: (78° 2' 5.5"N, 33° 52' 48"W)

Formatted: Highlight

Deleted:

Page Break

Deleted:

... [2]

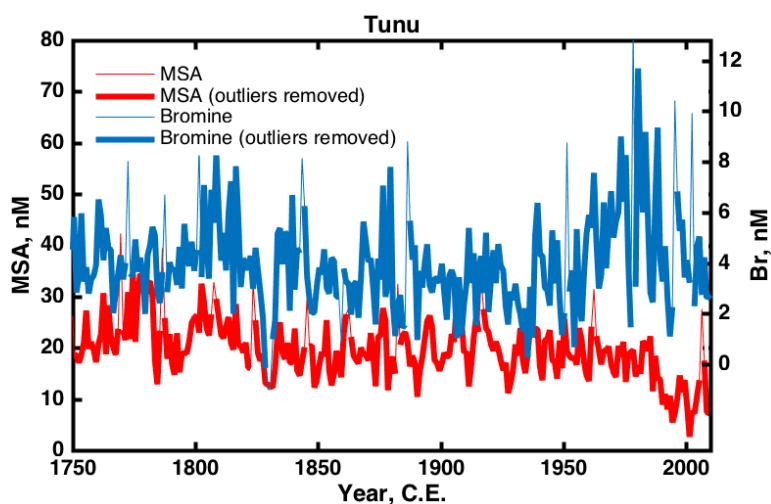
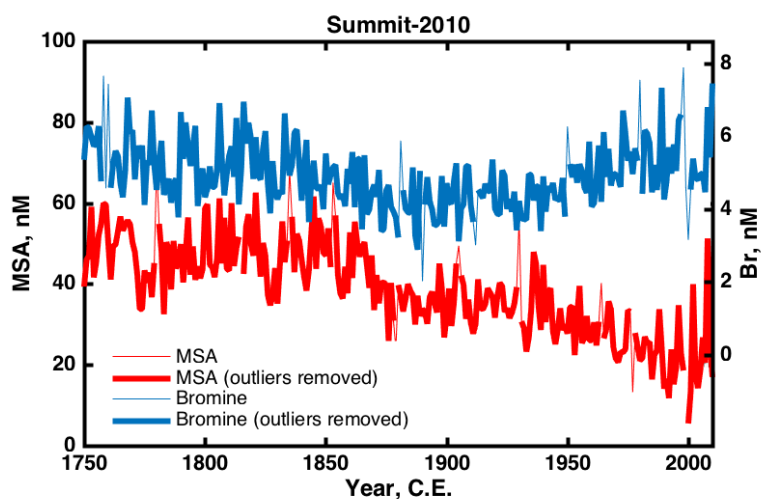
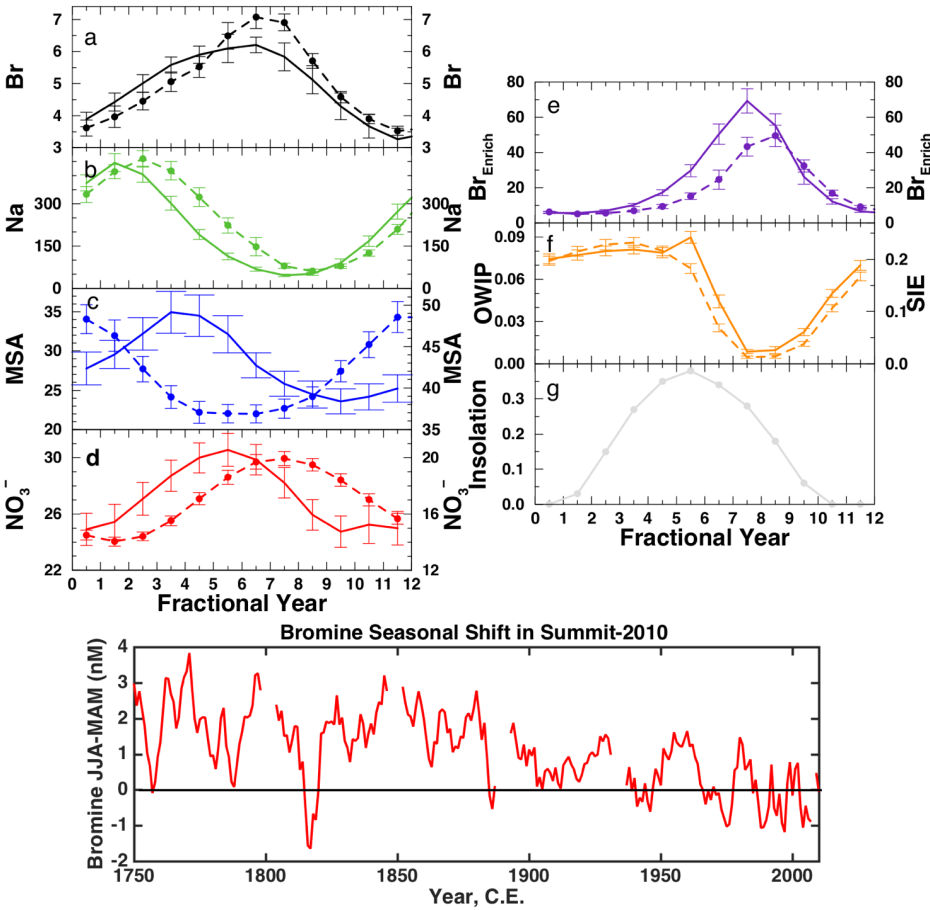


**Figure 2.** Annual record of bromine (thin blue) and MSA (thin red). Annual record of bromine (thick blue) and MSA (thick red) with outlying spikes removed using a 25 year running average filter described by Sigl et al. (2013). All records were fit with a 3 step linear regression and the results of the fits which

l43 identify the timing of inflection points are summarized in Table S1. The time-series have been plotted  
l44 to match the signal variability in the preindustrial era (1750-1850 C.E.).  
l45



148 **Figure 3.** Upper plots: Average seasonal cycle of species in the Summit-2010 ice core. The left-hand Y  
149 axes are associated with the solid lines, and the right-hand Y axes associated with the dashed lines.  
150 Dashed lines (a-e): Average seasonal cycle from depths 43.5 – 87.3 m (years 1742-1900). Solid lines  
151 (a-e): Average seasonal cycle from 0-43.5 m (years 1900-2010). Error bars indicate the standard error  
152 of the monthly value. (a) Total bromine, (b) total sodium, (c) MSA, (d) nitrate. Units for (a-d) are nM.  
153 Note that the seasonal cycle in bromine appears to broaden in the 1900-2010 period (see lower panel).  
154 Note also that the MSA maximum shifts from spring in the shallowest part of the ice core (solid line) to  
155 winter in the deepest part of the ice core (dashed line) due to post-depositional effects (see Fig. S1). (e)

Deleted: S3

157 Average seasonal cycle in bromine enrichment (relative to sea salt sodium, see Eq. (4)). (f-right) The  
158 sea ice extent ( $\text{SIE, } \times 10^6 \text{ km}^2$ ) within an area of the East Greenland coast [ $70^\circ\text{--}63^\circ \text{ N}$ ,  $15^\circ\text{--}45^\circ \text{ W}$ ]. (f  
159 – left) Area of open water within the sea ice pack ( $\text{OWIP, } \times 10^6 \text{ km}^2$ ) for the area defined by SIE. (g)  
160 Solar insolation at 12 GMT at the latitude of Summit ([eosweb.larc.nasa.gov](http://eosweb.larc.nasa.gov)). Lower plot: Broadening  
161 of bromine seasonal cycle in the Summit-2010 ice core. The difference between the summer and spring  
162 bromine signal (JJA-MAM) was monitored over the length of the entire ice core. In the preindustrial  
163 era (pre-1850) bromine peaks in summer; realised as positive values of JJA-MAM. After 1900 there is  
164 a marked broadening of the seasonal signal towards spring and by ~1970 the seasonal signal maximum  
165 is routinely shared between summer and spring realised as an averaged JJA-MAM of approximately  
166 zero.  
167

Deleted: ] that shows highest correlations to MSA (see Fig. 6),

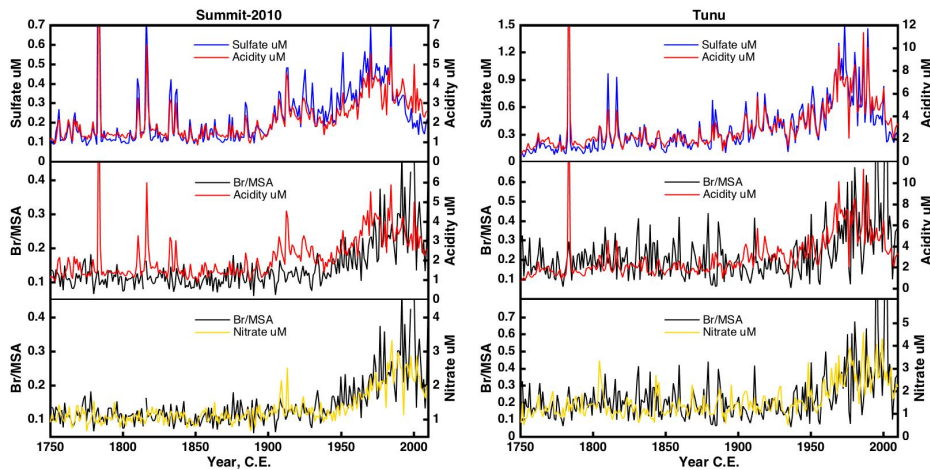


**Figure 4.** Comparison between the measured total sulfur (shown as sulfate) and acidity records from each ice core (top panels). The acidity record is dominated by the influence of the sulfur species until the early 21<sup>st</sup> century when the  $\text{NO}_x$  pollution remains elevated whilst anthropogenic sulfur sources are depleted resulting in a slight relative elevation of the total acidity relative to total sulfur concentrations. The large spikes in the acidity and sulfur records are identified as volcanic events. The ice core records cover the period of the 1783 Laki eruption as well as the Unknown 1909 eruption and Tambora eruption (Indonesia) in 1815 (Sigl et al., 2013). Comparison between Br/MSA and total acidity (center panels) and nitrate ( $\text{NO}_3^-$ , bottom panels) measured in the ice cores. The Br/MSA ratio follows the total acidity record closely except where the record is dominated by the sulfur component (e.g. early 1900s). Of the two major acidic species the Br/MSA follows the nitrate most closely at both ice core sites.

Deleted: <sp><sp>

Formatted: English (US)

Deleted: NO<sub>x</sub>

Deleted: ph



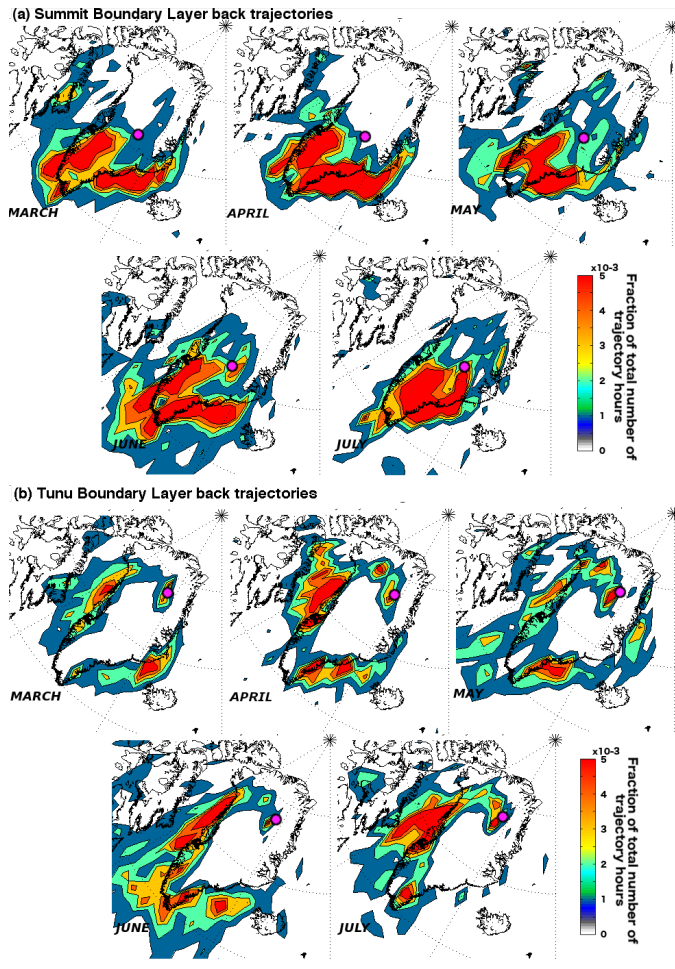
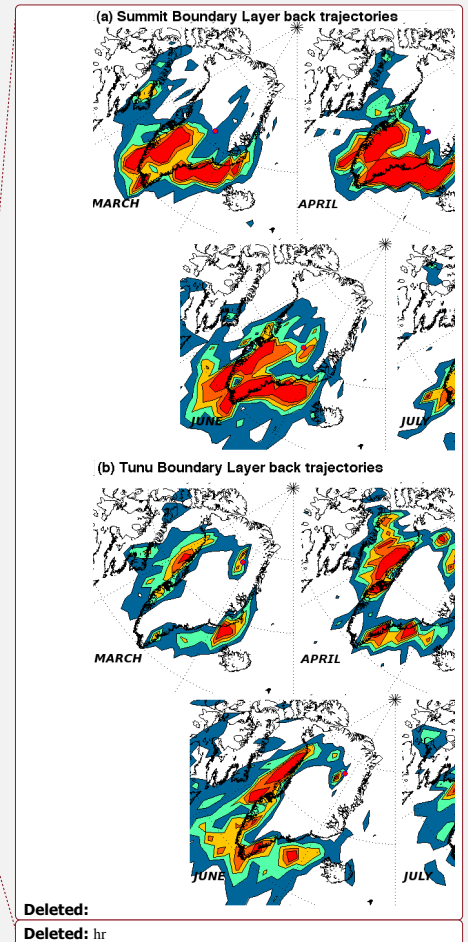


**Figure 5.** Air mass back trajectories from the (a) Summit-2010 and (b) Tunu ice core sites over the period 2005-2013 C.E. Maps display the fraction of the total number of trajectory hours (ranging between 21400-25500 hr month<sup>-1</sup>) spent at altitudes under 500 m. Back trajectories were allowed to travel for 10 days. New trajectories were started every 12 hours. Map grid resolution is 2°x 2°. Ice core locations are shown by a pink circle. Maps show that air masses consistently arrive at Summit from the SE Greenland coast with a smaller contribution from the SW coast. Air masses consistently arrive at Tunu from the western Greenland coast with a smaller contribution from the SE and NE coast. The air



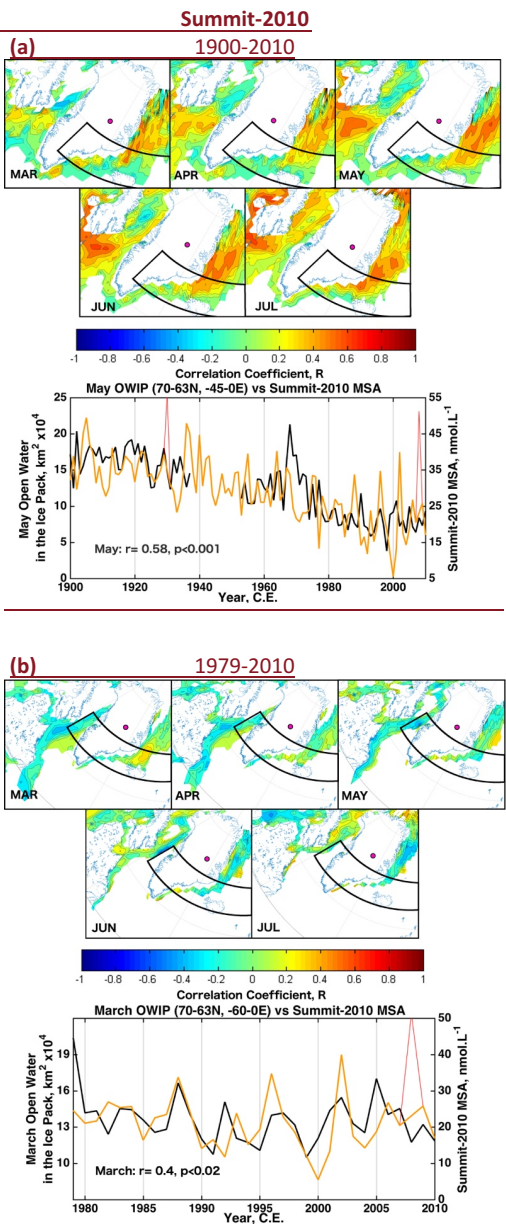
Deleted:  
Deleted: hr

198 mass originating from the NE coast is most dominant in May and comparison with the total vertical  
199 column profile (Fig. [S8](#)) shows it is confined to lower altitudes unlike those from the west coast.  
200

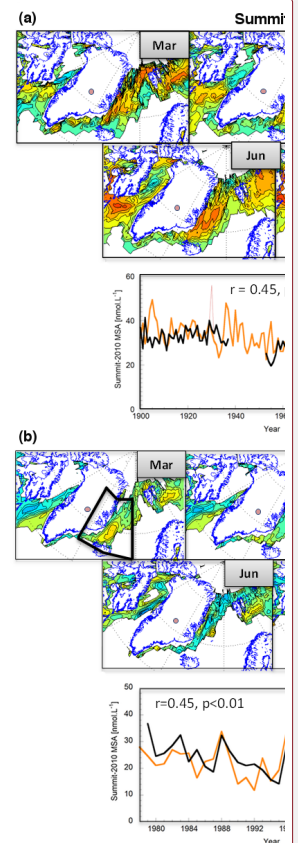
Deleted: S4

202  
203  
204  
  
205  
206  
207  
  
208  
209

Deleted: .  
Formatted: Justified



211 **Figure 6. Upper plots:** Correlation maps of monthly sea ice concentration (SIC) derived from the  
 212 Summit-2010 ice core. (a) HadISST1 ICE dataset from 1900-2010 C.E. correlated with annual records  
 213 of MSA. Outliers were removed from the MSA records before the correlations were performed to  
 214 prevent distortion of the correlations. Month labels indicate the month of SIC compared with the annual  
 215 MSA value. Only locations that showed a SIC variability greater than 10% and have a significant  
 216 correlation (t-test,  $p < 0.05$ ) are displayed. The area of sea ice that is the likely source of MSA (as  
 217 indicated by the air mass trajectories) are outlined in black [70°–63°N, 0°–45°W]. (b) As for (a) but  
 218 focused on the satellite period 1979-2010 C.E. and the outlined area covers [70°–63°N, 0°–60°W].  
 219 Lower plots: The correlation between the area of Open Water within the Ice Pack (OWIP) calculated  
 220 within the black outlined areas shown on the upper maps and the annual MSA records (red, outliers  
 221 removed - orange). Summit-2010 MSA shows a significant, positive correlation with the amount of  
 222 OWIP during spring within the integrated regions over both time periods. The highest correlations were  
 223 found for March over the 1979-2010 period and May for the 1900-2010 period. In (b) the MSA source  
 224 region was enlarged to [78°–63°N, 0°–60°W] as this increased slightly the March OWIP/MSA  
 225 correlation (from 0.38 to 0.4).



Deleted:

Formatted: Justified, Space Before: 0 pt, Tabs: 8.5 cm, Left

Deleted: 2

Deleted: .

Deleted: -

Deleted:

Deleted: 15

Deleted:

Deleted: Graphed is the

Deleted: of open water in the sea ice in this region

Deleted: ,

Deleted: ) overlaid

Deleted: (b) As for the upper panel but focused on the satellite period 1979-2012 C.E.

239

240

241

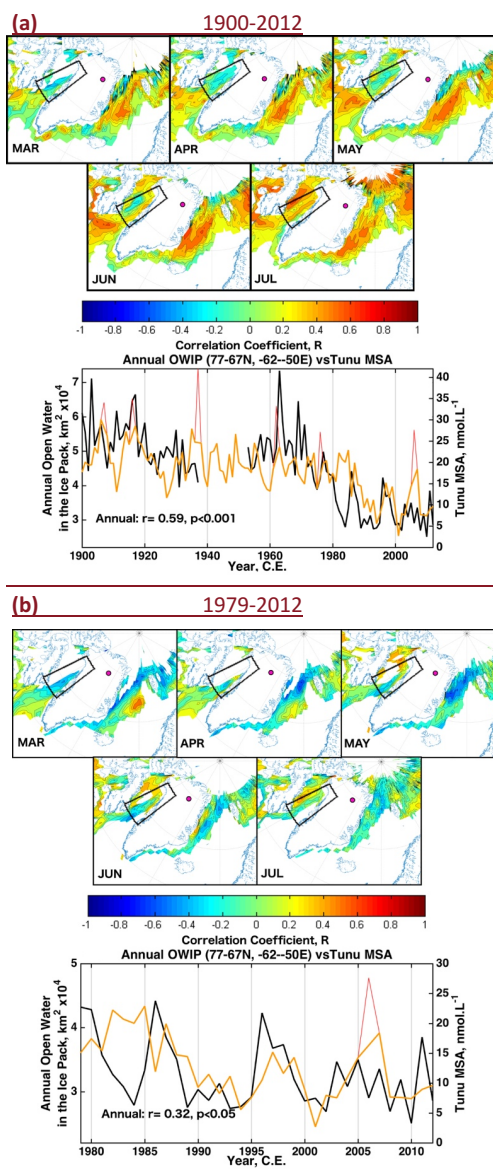
242

243

244

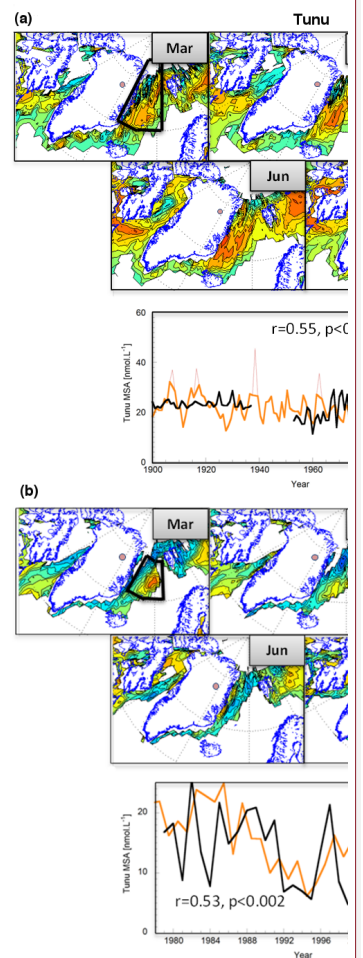
245

Tunu



Deleted: region.

Page Break



Formatted: Font:(Default) Times New Roman, Not Bold

**Figure 7. Upper plots:** Correlation maps of monthly sea ice concentration (SIC) derived from the Tunu ice core. (a) HadISST1 ICE dataset from 1900-2012 C.E. correlated with annual records of MSA.

249 Outliers were removed from the MSA records before the correlations were performed to prevent  
250 distortion of the correlations. Month labels indicate the month of SIC compared with the annual MSA  
251 value. Only locations that showed a SIC variability greater than 10% and have a significant correlation  
252 (t-test,  $p < 0.05$ ) are displayed. The area of sea ice that is the likely source of MSA (as indicated by the  
253 air mass trajectories) are outlined in black [77°– 67°N, 62°–50°W]. (b) As for (a), but focused on the  
254 satellite period 1979-2012 C.E. Lower plots: The correlation between the area of Open Water within  
255 the Ice Pack (OWIP) calculated within the black outlined areas shown on the upper maps and the annual  
256 MSA records (red, outliers removed - orange).  
257

Deleted: .

Deleted: -

Deleted: 80°– 73°

Deleted: 20°– 0°

Deleted: Graphed is the area of open water in the sea ice in this region (OWIP, black) overlaid on the annual MSA record (red, outliers removed - orange). Like in the Summit-20101 ice core, Tunu MSA also shows a significant, positive correlation with the amount of OWIP during spring but the correlation is highest when MSA is compared to the annual OWIP in the source region.

Deleted: the upper panel

Deleted: Again MSA shows a significant, positive correlation with the amount of OWIP during spring at both sites. During the satellite period the

Deleted: OWIP

Deleted: MSA concentrations at Tunu is greatly increased when a second, closer region is also included in the integration [80°–73° N, 20° –0° W].

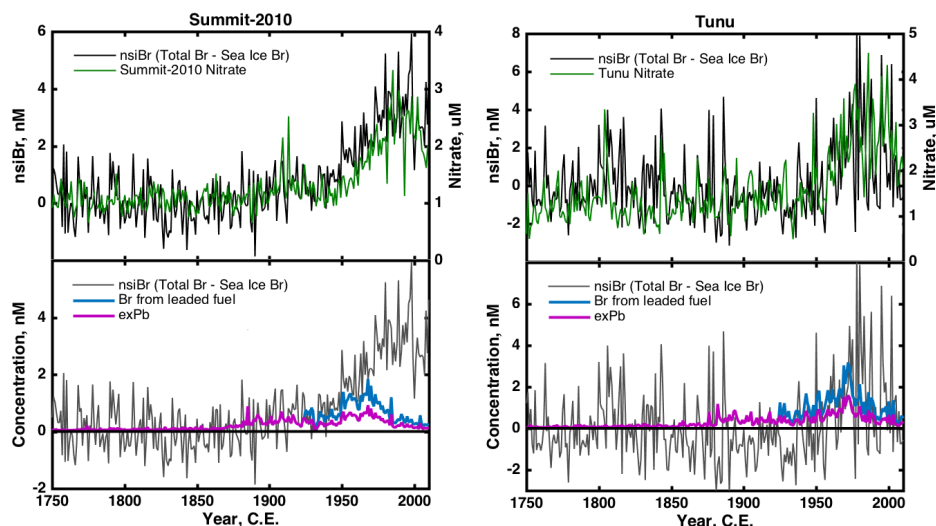


**Figure 8.** Upper panels: Comparison between bromine in excess of what is expected from a purely sea ice source (nsiBr, black) and nitrate. The temporal similarities between the nitrate and nsiBr records are high and indicate that nitrate is a likely driving force for the enhanced release of bromine species from sea ice sources. Lower panels: Comparison between the calculated nsiBr record and excess lead (exPb, purple) measured in the ice cores. The lower panels also show the upper limit to the amount of bromine that could be derived from leaded fuel combustion by assuming exPb:Br ratio of 1:2 after 1925 (blue). After 1970, when world consumption of leaded gasoline began to fall, nsiBr concentrations continued to rise at both ice core sites far above the concentrations that could be explained by leaded gasoline sources.

Deleted: ... [4]

Deleted: measurements of excess lead (exPb, purple shading) and

Deleted: the preindustrial (1750-1880) Br/MSA relationship (exBr

Deleted: ). Between 1925-1940 world-wide leaded gasoline sources contained a Pb:Br molar ratio of 1:2 (aviation fuel). After 1940 only Russia continued to use

Deleted: 1:2 ratio in their leaded fuel whilst the rest of the world changed to a 1:1 ratio. The green shading shows an estimate

Deleted: from leaded fuel combustion over the 1925-1940 period (relative to the exPb concentrations).

Deleted: blue shading shows

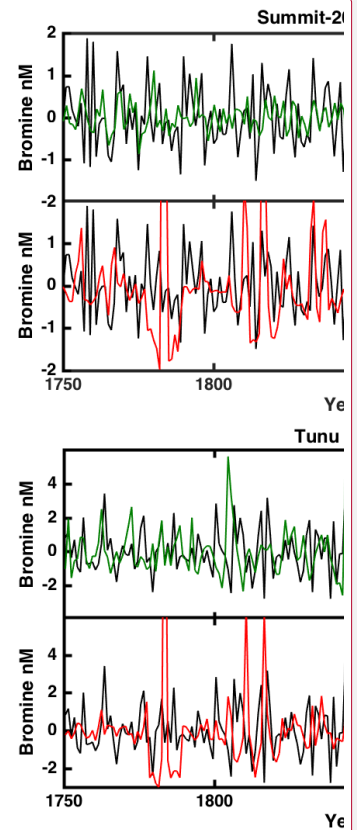
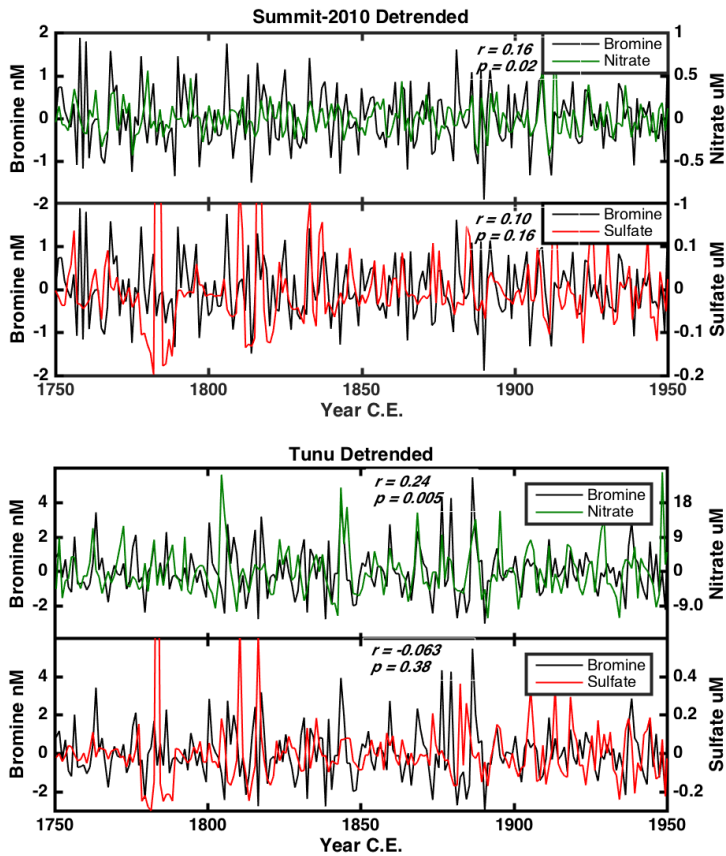
Deleted: (relative to exPb)

Deleted: 1940.

Deleted: exBr

Formatted: Font:(Default) Times New Roman, Not Bold





Deleted:

**Figure 9.** High frequency comparison between the annual bromine, nitrate and sulfate records measured in the ice cores. Each series has been detrended with an 11 year running average before comparison to remove the low frequency changes in each record. The correlation is highest between bromine and nitrate at both sites. The r-value for bromine versus nitrate at Summit increases in significance ( $r = 0.24$ ,  $p = 0.001$ ) when the entire period (1750-2010) is considered. At both sites there is a close relationship between the variability in the nitrate and bromine due to their intimate relationship during emission from the sea ice, transport and deposition onto the snow pack. The correlation between sulfate (or indeed bulk acidity) and bromine is not significant over any of the time periods shown at either site. Particularly

Deleted: significant

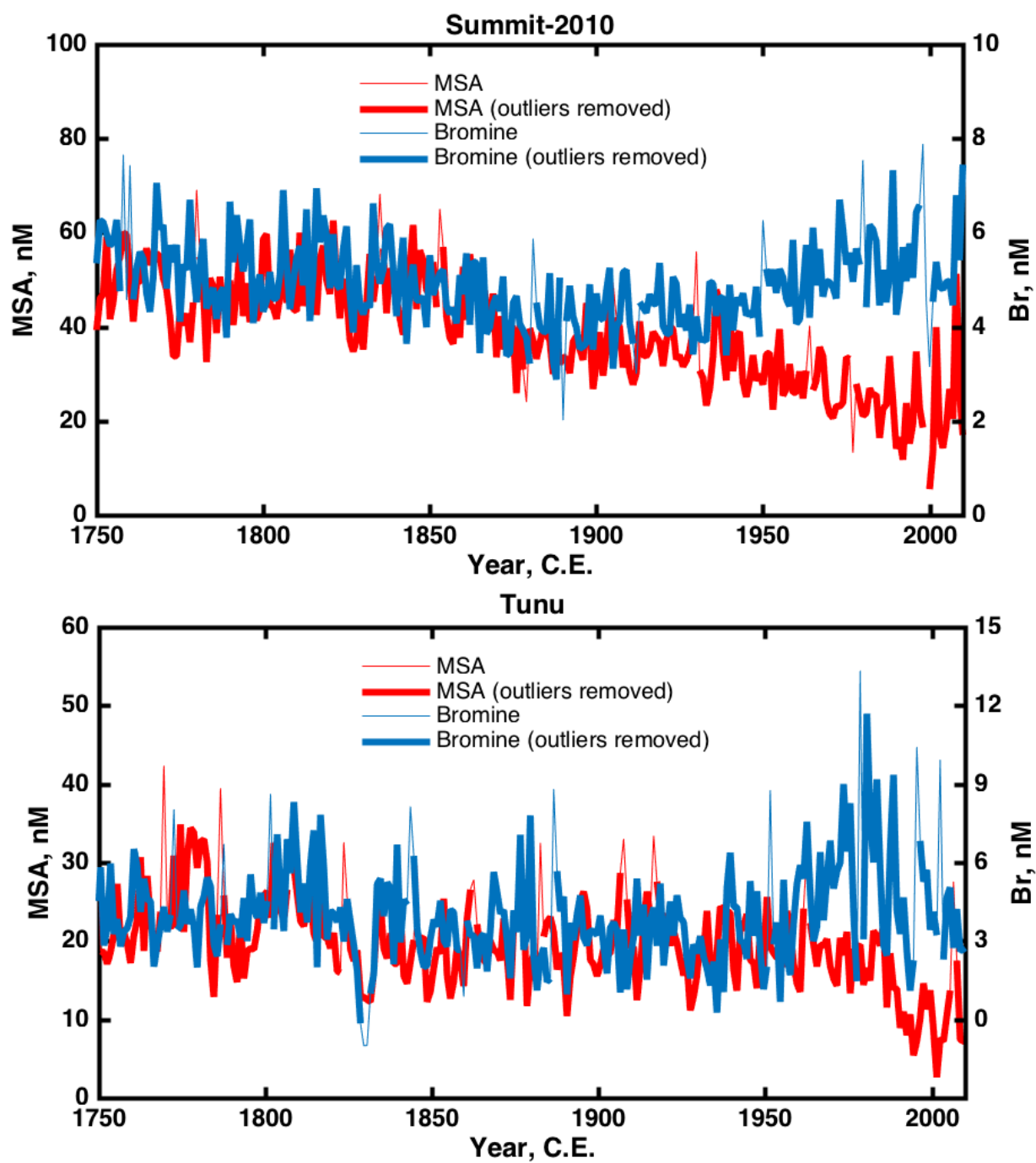


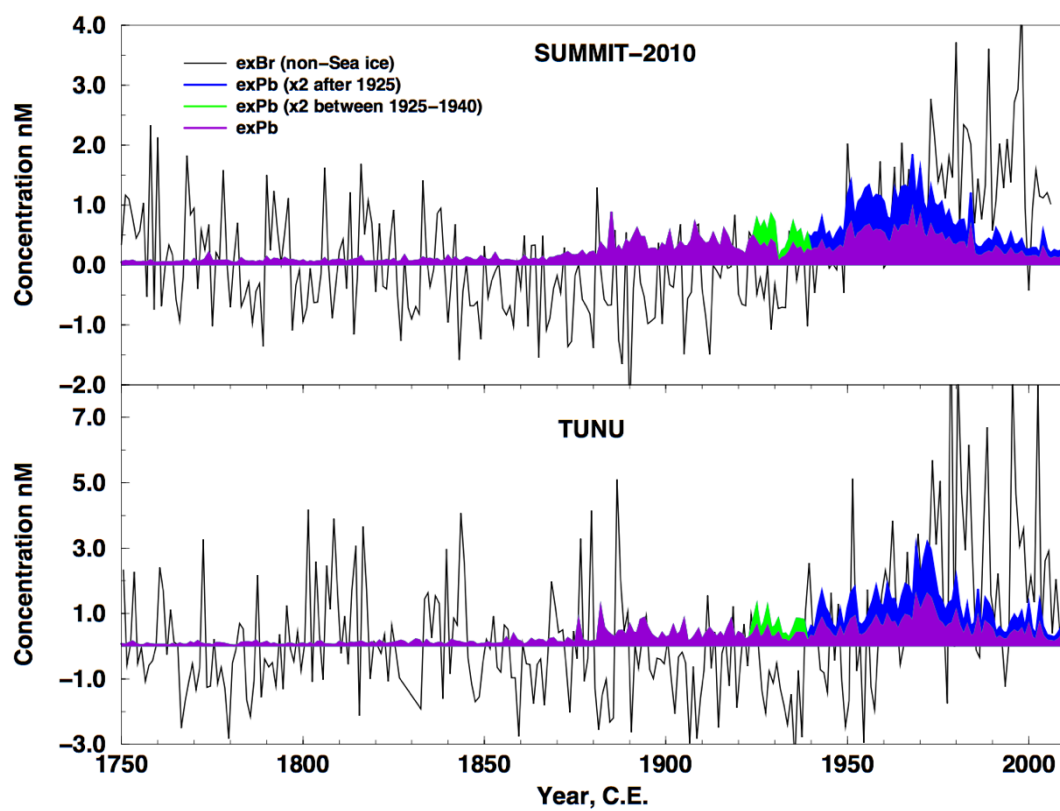
316 evident is the non-response of the bromine signal to the sulfur rich volcanic events as described in  
317 Sect.4.2.2.  
318

Formatted: Left, Space Before: 0 pt, Line spacing: single

Bromine has also been suggested as a possible proxy for sea ice conditions, however the timing of the largest bromine aerosol flux, in summer, does not coincide with the largest growth or extent of new sea ice. Sea ice begins to increase only at the end of summer as the fractures in the ice cover are re-laminated and the ice edge begins to advance southward (see Fig. 3f).

So what is the summer-time source of bromine? What is the cause of the increase in spring-time bromine explosion events in the industrial era? (see Fig. 3, lower panel) and why does the bromine record deviate from the sea ice proxy record (MSA) around the same time? Possible sources of bromine and the factors which may effect the resultant bromine flux are discussed below.





Supplementary figures and tables

**Table S1.** Summary of timings of each inflection in the 3-step linear regression of annual bromine and MSA at Summit and Tunu. Regression was performed on the data sets with outliers removed as described in Fig. 2. The signs indicate the direction of the inflection in the record, errors are  $2\sigma$ .

Timing of inflection (Year, C.E.)

	Infl. 1		Infl. 2		Infl. 3		Infl. 4
	Br	MSA	Br	MSA	Br	MSA	Br
Summit-2010	(-)1819 ±22	(-)1854 ±12	(+)1879 ±22	(+)1878 ±12	(+)1932 ±10	(-)1930 ±16	(-)1974 ±20
Tunu	(-)1842 ±22	(-)1812 ±12	(+)1857 ±24	(+)1821 ±21	(+)1944 ±18	(-)1984 ±4	(+)1966 ±20

Formatted: Level 1

Deleted: ... [1]

1 **Table S2.** Summary of the average aerosol concentrations as determined by the 3-step linear regression of  
2 annual bromine and MSA at Summit and Tunu displayed in Fig. 2. The duration of each step in concentration  
3 is bracketed by the inflection points summarized in Table S1. Concentrations are in units of nM. MSA did not  
4 show a stable period after the third infection in the series and so was not assigned a concentration value for  
5 ‘Step 3’. Errors represent  $2\sigma$  in the concentration value.

6

	Concentration (nM)				
	Step 1		Step 2		Step 3
	Br	MSA	Br	MSA	Br
Summit-2010	5.4±0.2	48±1	4.2±0.2	36±2	5.5±0.3
Tunu	4.2±0.3	25±1	3.2±0.3	21.2±0.7	4.8±0.5

Formatted: Centered

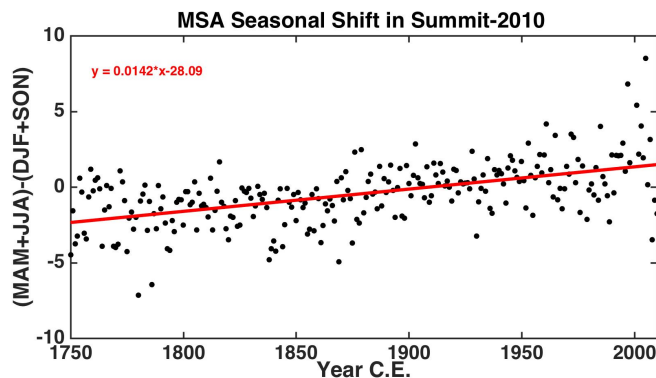
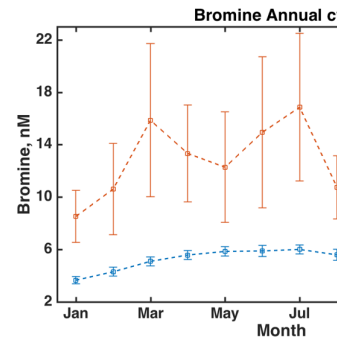


**Figure S1.** Illustration of the shift in the seasonal MSA peak along the length of the Summit-2010 ice core. The difference in amplitude between the spring/summer and winter/fall MSA signal each year was calculated ((MAM+JJA)-(DJF+SON)) and observed to shift linearly along the length of the ice core. At the shallowest, part of the ice core the positive values show the MSA peak appears in the spring/summer whilst in the deepest and oldest part of the ice core the signal has shifted to a winter/fall annual maximum. This phenomenon has previously been attributed to annual salt gradients within the ice core driving the migration of the MSA toward the higher salt location, winter (Mulvaney et al., 1992; Weller, 2004).

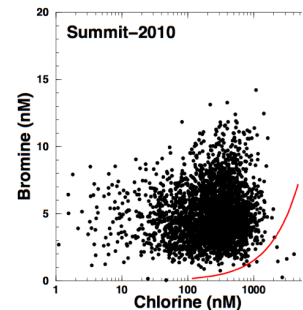
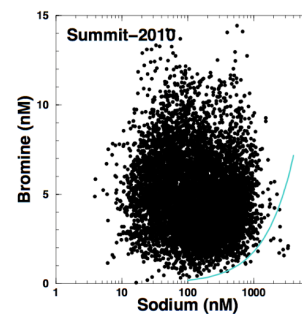


Deleted:

Moved down [1]: Figure S1.

Moved down [5]: Figure S3.

Moved (insertion) [1]



Deleted:

Moved down [3]: Figure S2.

Deleted: Monthly values of bromine, sodium and chlorine compared with their sea water ratio (coloured lines). At both sites, both the (a) Br/Na and (b) Br/Cl lie predominantly above the sea water ratio.

Moved down [4]:  $([Br]/[Na])_{\text{seawater}} = 1.793 \times 10^{-3}$ ,  $([Br]/[Cl])_{\text{seawater}} = 1.539 \times 10^{-3}$ .

Deleted:

Deleted: icecore

Moved down [6]: Figure S4.

Formatted: English (US)

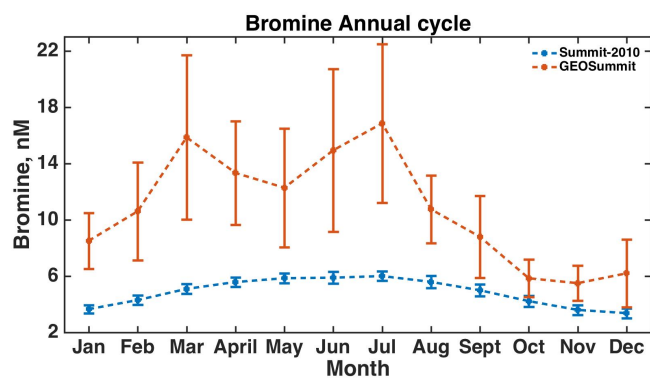


**Figure S2.** Comparison between the annual cycle in inorganic Br measured at Summit from snow samples taken as part of the GEOSummit project (2007-2013) and in the Summit-2010 ice core (1900-2010). The snow samples were analysed for inorganic Br on the same system used to measure the ice core records. The results of the snow samples support the observation from the ice cores that the maximum flux of Br is in summer with a possible secondary peak in spring. The error bars represent  $1\sigma$ .

Moved (insertion) [3]

Moved (insertion) [2]



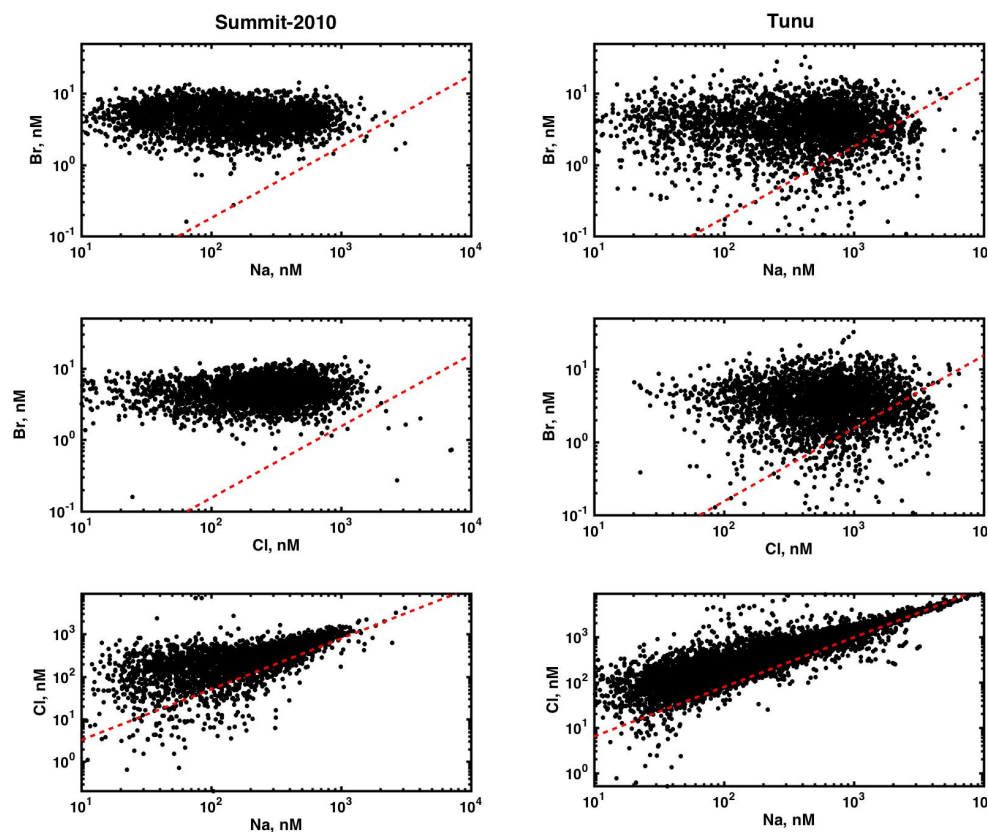


**Figure S3.** Monthly values of bromine, sodium and chlorine compared with their sea water ratio (red). At both sites, both the Br/Na and Br/Cl lie predominantly above the sea water ratio, whilst Cl/Na shows only a small Cl enrichment which increases at small sodium concentrations. At Tunu, 11% and 12% of the points show bromine depletion relative to Na and Cl, respectively.  $\left(\frac{[\text{Br}]}{[\text{Na}]}\right)_{\text{seawater}} = 1.793 \times 10^{-3}$ ,  $\left(\frac{[\text{Br}]}{[\text{Cl}]}\right)_{\text{seawater}} = 1.539 \times 10^{-3}$ ,  $\left(\frac{[\text{Cl}]}{[\text{Na}]}\right)_{\text{seawater}} = 1.165$

Moved (insertion) [5]

Moved (insertion) [4]

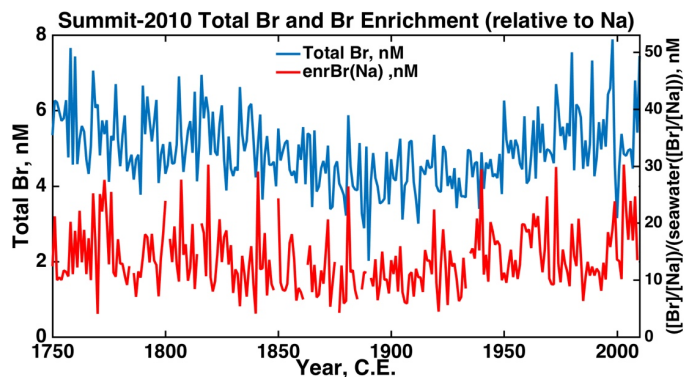


**Figure S4.** Total bromine and bromine enrichment (relative to sodium) from the Summit-2010 ice core. The time-series have been plotted to match the signal variability in the preindustrial era (1750-1850 C.E.).

Moved (insertion) [6]

Formatted: English (US)

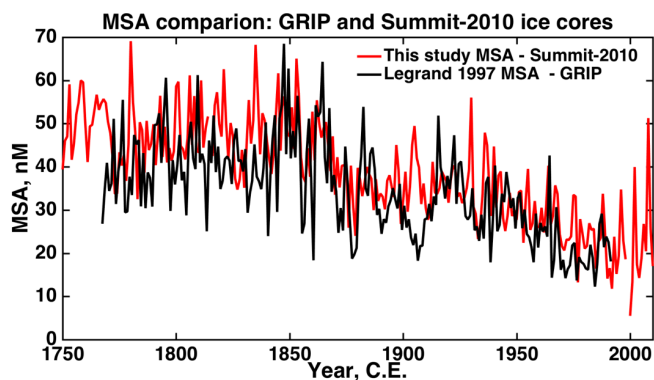


**Figure S5.** Comparison between the MSA record obtained from the GRIP ice core (Legrand et al., 1997) in 1993 and the Summit-2010 ice core from this study. The Summit-2010 ice core drill-site ( $72^{\circ}20'N$   $38^{\circ}17'24''W$ ) is located 35 km SW of the GRIP ice core drill-site ( $72^{\circ}34'N$ ,  $37^{\circ}38'W$ ). The GRIP MSA was measured in discrete samples using ion chromatography compared with the Summit-2010 ice core which was measured using the new technique of continuous melting of the ice core combined with continuous analysis by electrospray triple-quad mass spectrometry (as described in the text). The tight overlap between low frequency trend of the two series demonstrates that the new, continuous measurement technique is able to achieve a comparable accuracy in MSA concentration measurements to the discrete technique. It also demonstrates that negligible amounts of MSA are being lost during the continuous melt method. Discrepancies between the high frequency features of the two records is expected as the measurement resolution of the continuous method is much higher than the discrete method and the two records are from different ice core sites.

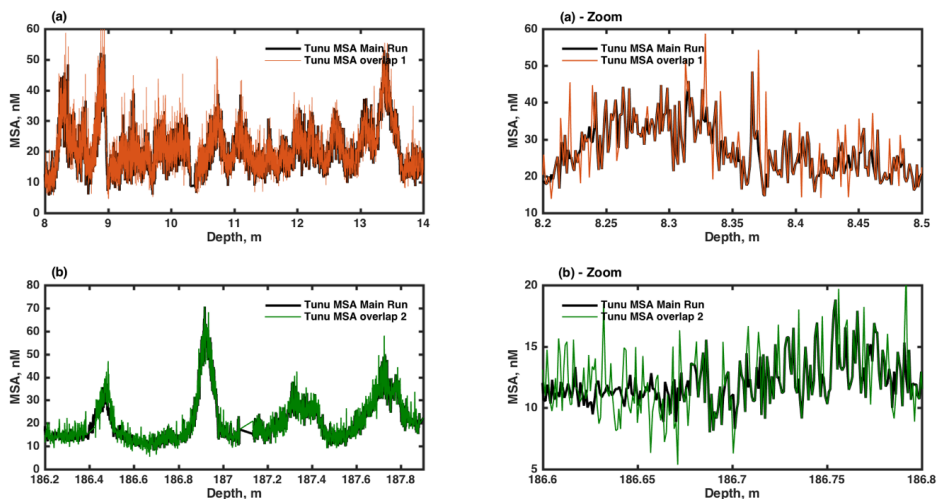


**Figure S6.** Demonstration of the reproducibility of the MSA online, continuous measurements performed on the Tunu ice core. Two different depths of the Tunu ice core are shown where the replicate analysis was performed by melting a secondary stick of ice cut from the same ice core and overlapping in depth: (a) Six ‘overlap’ ice cores were melted sequentially to replicate the MSA record over the depth 8-14 m.(b) Two ‘overlap’ ice cores were melted sequentially over the depth 186.2-187.9 m. Zooming in on a small section of the record at each depth demonstrates that the high frequency signal is real (not noise) and well replicated by the continuous MSA technique.

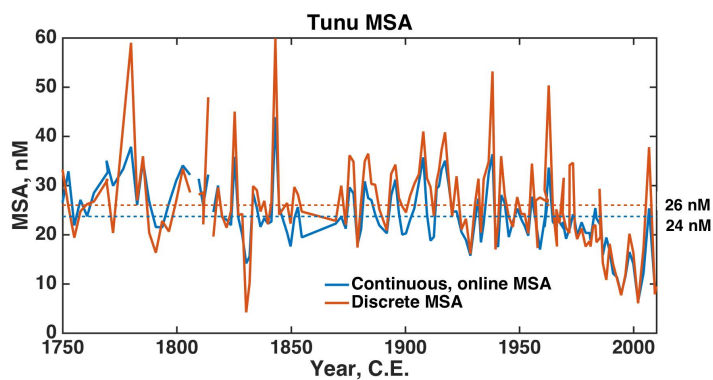


**Figure S7.** Comparison between discrete and continuous, online measurements of MSA measurements from the Tunu ice core samples. The discrete samples were collected as the continuous measurements were performed by directing part of the sample stream into an auto-sampler collection system just before they entered the analyzer. The samples were then frozen and later measured using ion chromatographic separation and the ESI/MS/MS detection. In this plot the continuous data have been averaged over the same depth range covered by each discrete sample and then both series plotted as the average age over that depth range. Over the 1750-2012 period the Tunu discrete measurements were, on average, 7% higher than the online measurements (dashed lines indicate average values over the 1750-2012 period). Both the discrete and continuous samples experienced identical conditions from ice melt to collection so the reason for offset in measured concentration is likely due to differences in post-processing of the data.

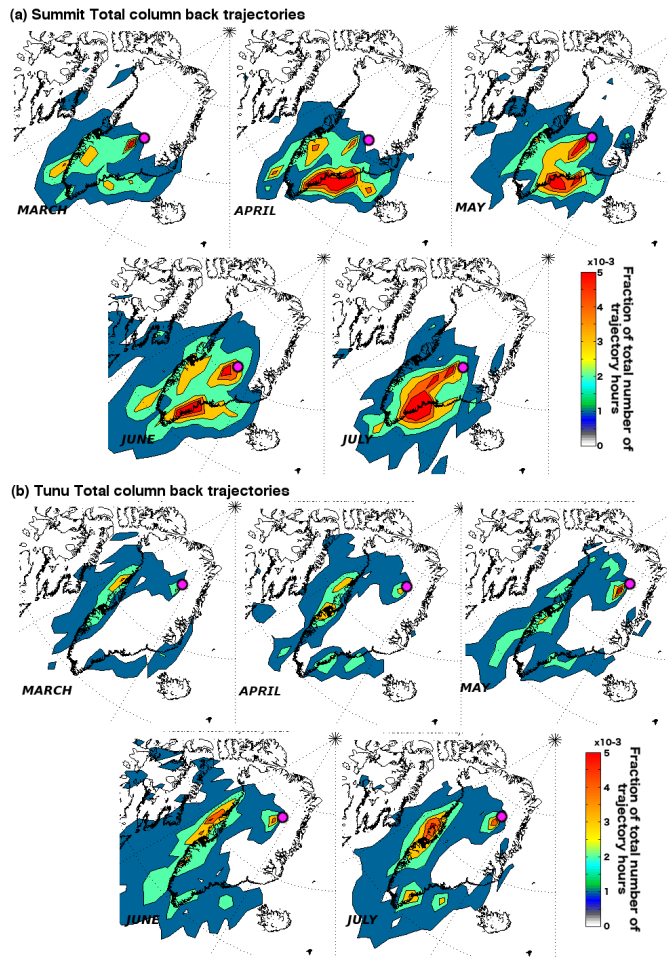


**Figure S8.** Total column air mass back trajectories from the (a) Summit-2010 and (b) Tunu ice core sites over the period 2005-2013 C.E. Maps display the fraction of the total number of trajectory hours ( $\sim 100000$  hrs month<sup>-1</sup>) spent within the total vertical column (under 10000 m). Back trajectories were allowed to travel for 10 days. New trajectories were started every 12 hours. Map grid resolution is 2°x2°. Ice core locations are shown by a pink circle. Maps show that air masses consistently arrive at Summit from the SE Greenland coast with a smaller contribution from the SW coast, consistent with the trajectories seen in the boundary layer (Fig. 5). Air masses consistently arrive at Tunu from the western Greenland coast with a smaller contribution from the SE.

Deleted: hours

Deleted: 6

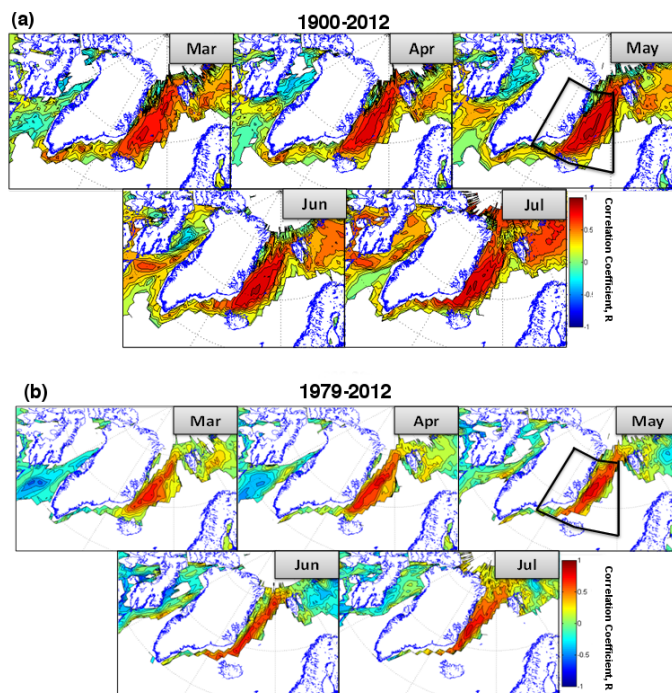


**Figure S9.** Autocorrelation maps of SIC during (a) the extended era (1900–2012 C.E.) and (b) satellite era (1979–2012 C.E.). Monthly SIC values were compared with the average SIC record from the area which shows the high positive correlation to the Summit-2010 MSA record (outlined in black in Figs. 6a, 6b). There is clearly a negative correlation between sea ice on the east and west coast which is seen over both era from March through to May, but the relationship turns positive in June and July over the extended time period (1900–2012 C.E.)

Formatted: Centered

Deleted: S5

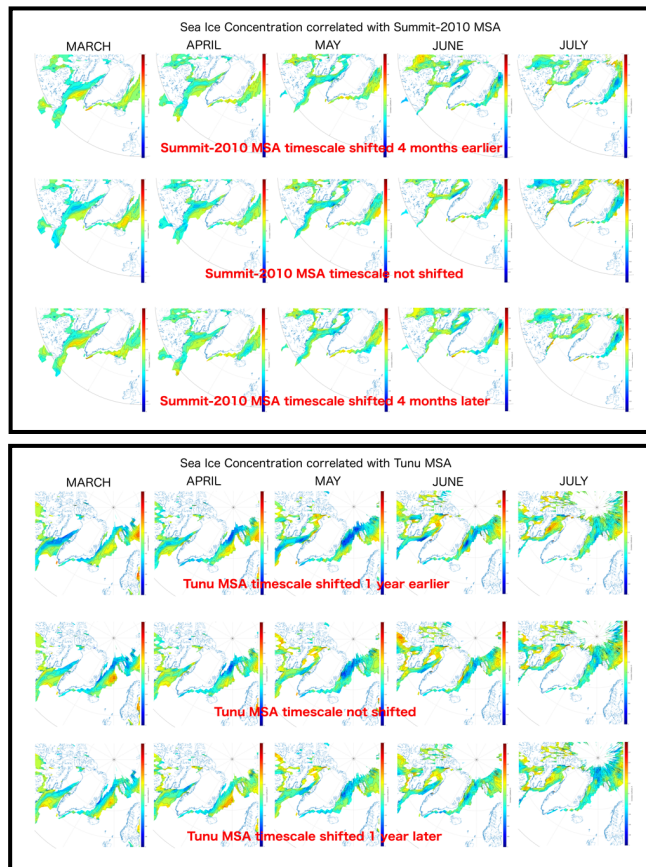


**Figure S10.** Analysis of the effect of errors in the ice core timescales on the correlation between the site MSA record and the local sea ice concentrations (SIC). By shifting the dating of the MSA records to either extreme of the dating error estimate and replotting the SIC correlation plots (Figs. 6 and 7) it is clear the error in the dating of the MSA records does not affect the sign of the correlations displayed on the maps but can have an affect on the magnitude of the correlation found in different locations. This is likely a result of the peaks in the MSA record being shifted in or out of temporal coherence with peaks in SIC at the different locations.



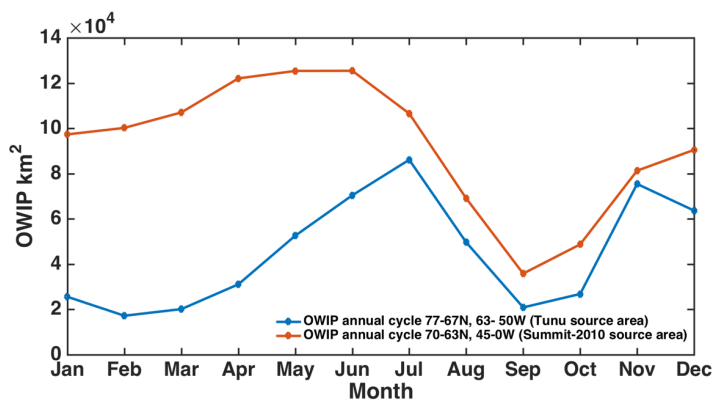


**Figure S11:** Annual cycle of open water in the ice pack (OWIP) within the aerosol source regions designated in Figs. 6 and 7. The annual cycle has been averaged over the period 1900-2012. The satellite period 1979-2012 shows the same temporal variability in OWIP at both sites but at reduced OWIP values.

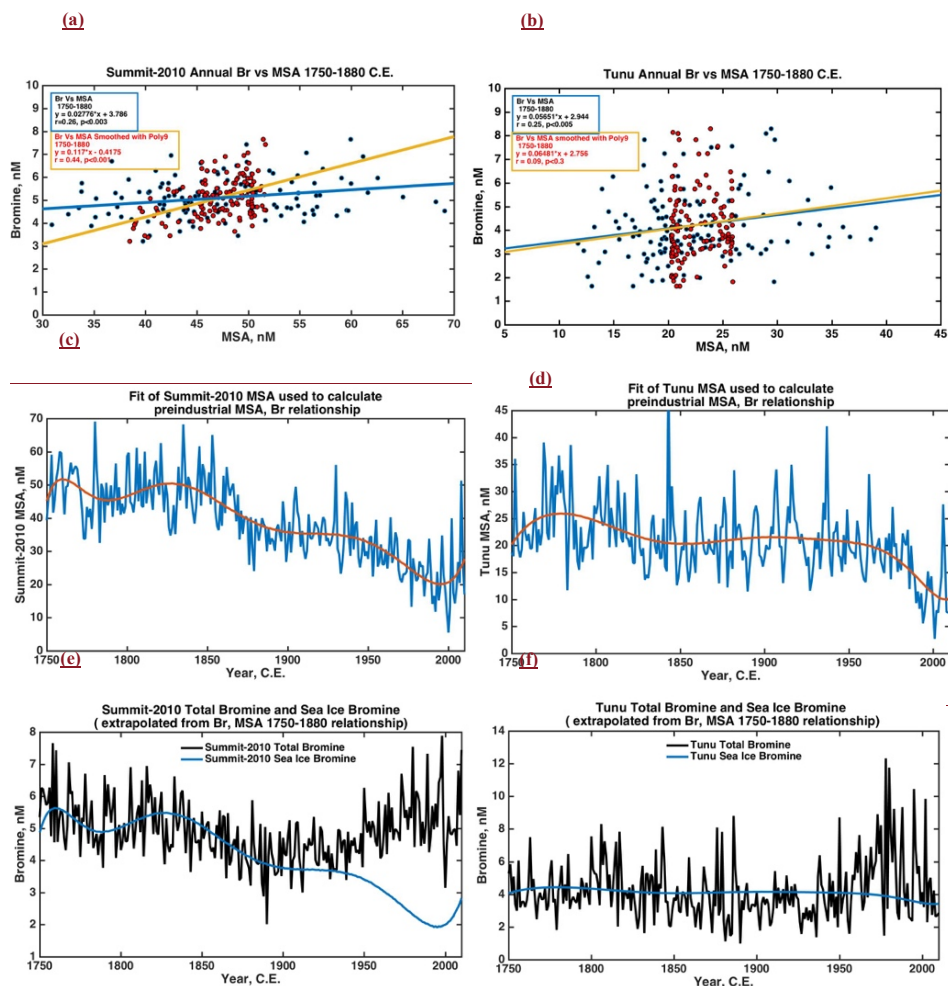


**Figure S12:** Summary of the technique used to determine nsIBr: the amount of Bromine in excess of what is expected from a purely sea ice source. (a,b) Blue dots, blue fit line: correlation plots between total bromine and total MSA in Summit-2010 and Tunu ice cores, respectively over the preindustrial period 1750-1880 C.E.. Red dots, yellow fit line: Correlation plots between total bromine and smoothed MSA time series shown in c and d. (c,d) Annual MSA record fit with 9th order polynomial. (e,f) Comparison between the total bromine record (black) and the bromine predicted from the smoothed MSA, Br linear relationship determined in a and b (blue) – the bromine from a purely sea ice source. The difference between the blue and black lines in panels

e and f is the amount of bromine in excess of what is expected from a purely sea ice source (nsiBr; see Fig. 8).

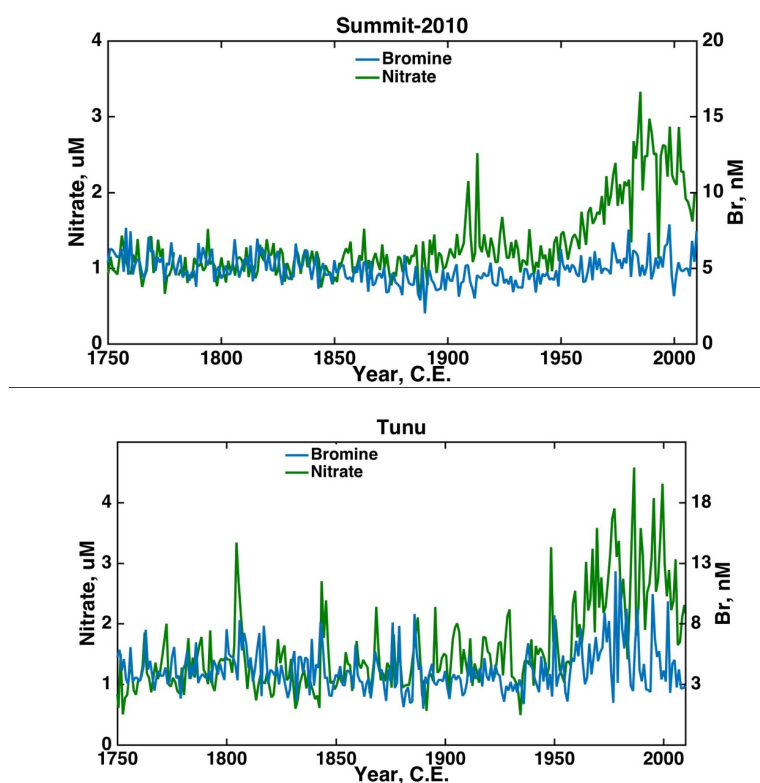


**Figure S13:** Comparison between nitrate and bromine records at both ice core sites. The time-series have been plotted to match the signal variability in the preindustrial era (1750-1850 C.E.). The difference between the two time-series is most dramatic at the Summit-2010 site because the sea ice record changes most dramatically at this site – and sea ice is the underlying driver of the bromine record.

Page 1: [1] Deleted	olivia maselli	25/08/2016 10:07 PM
---------------------	----------------	---------------------

Page 3: [2] Moved to page 3 (Move #1)	olivia maselli	25/08/2016 10:07 PM
---------------------------------------	----------------	---------------------

**Figure S1.**

Page 3: [2] Moved to page 3 (Move #1)	olivia maselli	25/08/2016 10:07 PM
---------------------------------------	----------------	---------------------

**Figure S1.**

Page 3: [3] Deleted	olivia maselli	25/08/2016 10:07 PM
---------------------	----------------	---------------------

